ADVANCED MATERIALS
www.advmat.de

Biopolymers Derived from Trees as Sustainable Multifunctional Materials: A Review

*Chao Liu, Pengcheng Luan, Qiang Li, Zheng Cheng, Pengyang Xiang, Detao Liu, Yi Hou, Yang Yang, and Hongli Zhu**

The world is currently transitioning from a fossil-fuel-driven energy economy to one that is supplied by more renewable and sustainable materials. Trees as the most abundant renewable bioresource have attracted significant attention for advanced materials and manufacturing in this epochal transition. Trees are composed with complex structures and components such as trunk (stem and bark), leaf, flower, seed, and root. Although many excellent reviews have been published regarding advanced applications of wood and wood-derived biopolymers in different fields, such as energy, electronics, biomedical, and water treatment, no reviews have revisited and systematically discussed functional materials and even devices derived from trees in a full scope yet. Therefore, a timely summary of the recent development of materials and structures derived from different parts of trees for sustainability is prsented here. A concise introduction to the different parts of the trees is given first, which is followed by the corresponding chemistry and preparation of functional materials using various biopolymers from trees. The most promising applications of biopolymer-based materials are discussed subsequently. A comprehensive review of the different parts of trees as sustainable functional materials and devices for critical applications is thus provided.

1. Introduction

The increasing demand for petroleum-derived materials and products has resulted in various environmental problems and shortages of these commodities.[1] Hence, the world is currently transitioning from an age depending on petroleum-based materials to one that is supplied by more renewable and sustainable resources.[2] The annual solar energy utilized by lignocellulose biomass, such as trees, grass, and agricultural feedstock, is ten times the total energy used by humans.[3] There is no doubt that lignocellulosic biomass will play an increasingly important role in our future sustainability.[4] Trees represent an abundant renewable source of lignocellulosic biomass, which is considered as a sustainable material. In addition, trees provide us with oxygen and remove carbon dioxide from the atmosphere via photosynthesis reactions.

The different parts of trees, including the trunk, leaf, flower, seed, and root, are all widely used in our society. Traditionally, trunk (accounts for 60% of the tree), mainly composed of bark, cambium and xylem, is the central part of the tree supporting, transporting of water, minerals and nutrients and protecting trees from disease, insects, and harsh environment. Trunk is widely used in our lives as constructing materials for buildings and furniture, combustion, manufacturing for paper, and many others. Leaves (account for 5% of the tree) supply energy and nutrition for the trees by transforming light energy into chemical energy, which is stored in carbohydrate molecules, such as sugars, via photosynthesis. Flowers, the reproductive organs of trees, attract insects for pollination and provide humanity various pigments. Seeds are the results of reproduction and serve as the propagule, which contain the genetics of a tree and food reservoirs in the form of cotyledons and endosperm. Some tree seeds have high medical value and can be used to extract oil. Roots (account for 20% of the tree) are fibrous-like, which can feed the entire tree and absorb nutrients and water from the soil and transport them to the trunk. Even though some of the aforementioned applications of tree parts can be backed in thousands of years, functional materials and devices have been centered in the recent decades for converting tree into high-value products.

Different parts of the tree have distinct applications due to the different concentrations of the component chemicals and different structures. Trunk from wood has a naturally hierarchical porous structure with aligned channels and numerous micro/nano pores. Inspired by the inherent properties and structure of wood, advanced applications of sustainable wood materials have boomed; for example, in sustainable energy storage,[5] biodegradable flexible electronics,[6] solar steam generation,[7] and natural energy harvesting.[8] Wood is a natural composite material that is mainly composed of cellulose, lignin, and hemicellulose. These biopolymers have multiple functional groups,

C. Liu, P. Luan, Dr. Q. Li, P. Xiang, Dr. Y. Yang, Prof. H. Zhu
Department of Industrial and Mechanical Engineering
Northeastern University
360 Huntington Ave, Boston, MA 02115, USA
E-mail: h.zhu@neu.edu
Dr. Z. Cheng, Prof. D. Liu, Prof. Y. Hou
State Key Laboratory of Pulp and Paper Engineering
South China University of Technology
Guangzhou 510640, China
The ORCID identification number(s) for the author(s) of this article can be found under https://doi.org/10.1002/adma.202001654.

DOI: 10.1002/adma.202001654

making them suitable for chemical modification and reconfiguration. In addition to similar components as wood, the bark contains particular components with higher tannin content than other parts of tree. Flowers and leaves have high pigment contents that can be used to extract dyes. Recently, in the context of biorefineries, many sustainable and green fractionation techniques have been developed to enable the utilization of these biopolymers in large quantities in multiple industries. In addition, biopolymers derived from trees are considered as a kind of sustainable resource for developing advanced materials for use in high-tech fields, such as energy storage, flexible electronics, biomedicine, and water purification.

In the past years, several excellent reviews have discussed advanced applications of wood and wood-derived nanomaterials in different fields.[9,10] The relationships between the structure, properties, and applications of wood have also been summarized in detail in other comprehensive review articles.[10,11] However, recent advances in the use of each part of the tree for energy, biomedical, environment, and electronics have not been reviewed in detail yet. Understanding the fundamental function of different parts of trees is crucial for designing and manufacturing products for emerging applications. The aim of this review is to explore biopolymers derived from different parts of trees and their use in the development of sustainable functional materials and devices (as shown in **Figure 1**). This review will inspire research in biopolymer-based advanced materials and inspire new ideas to explore value-added high-value utilization of trees.

2. Structures and Chemical Components of Trunk

2.1. Hierarchical Structures of Trunk

Trunk is the predominant and most important part of the tree that human has used, for example, as firewood for heating, furniture, and construction. For industrial electricity generation, combustion of wood offers the advantages of biorenewability, abundant fuel source, competitive calorific value (18.5–22.0 MJ kg^{-1}), and low sulfur and nitrogen contents as compared with coal. The combustion of wood therefore represents a promising alternative to coal-fired power plants for reducing greenhouse gas emission and promoting the production of sustainable and renewable energy. In addition, bulk wood is a popular material for timber engineering and construction, as it is lightweight, has high strength, toughness, workability, and durability, and is a sustainable resource. The intrinsic mechanical strength of bulk wood that enables the engineering applications is a result of its macroscopic, microscopic, and molecular structures, including S1–S2–S3 layered cell walls with helical microfibrils, hydrogen bonding, and crystalline and inter-/intramolecular links. These characteristics give wood fiber viscoelastic characteristics. The unique hierarchical structure of wood, from the molecules to microscopic cell walls and macroscopic fibers, provides mechanical support to transfer the applied load until its ultimate failure strength, making wood a strong natural material for furniture and construction (**Figure 2**).

In addition to bulk use, wood has been cut into chips and blocks for emerging advanced materials and devices. The first

Chao Liu is currently an exchange Ph.D. student between Northeastern University and State Key Laboratory of Pulp and Paper Engineering in the South China University of Technology. His research focuses on bioderived multifunctional materials toward sustainable applications, including lignin nanoparticles for water treatment, high-performance bioderived solar stem devices, and cellulose-based lightweight structural materials for thermal management.

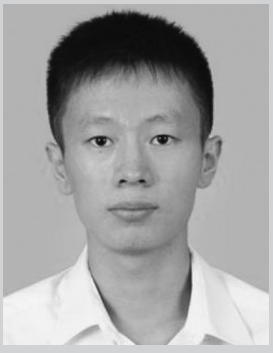

Pengcheng Luan is currently an exchange Ph.D. student between Northeastern University and State Key Laboratory of Pulp and Paper Engineering in the South China University of Technology. His research interests focus on the extraction and functional modification of lignocellulosic biomass, including eco-friendly delignification processes, lignocellulosic sorbent, and cellulose-based reverse electrodialysis devices. Furthermore, he is also interested in the industrial applications of cellulose in the field of pulp and paper manufacturing and environmental protection.

Hongli Zhu is currently an assistant professor at Northeastern University. Her group works on electrochemical energy storage, bioderived, bioinspired multifunctional materials, and emerging advanced manufacturing technologies. From 2012 to 2015, she worked at the University of Maryland as a research associate, focusing on the research of flexible nanopaper electronics and energy storage. From 2009 to 2011, she conducted research on materials science and processing of biodegradable and renewable biomaterials from natural wood at KTH Royal Institute of Technology in Sweden. Her expertise is on the research of energy storage (flow batteries, solid-state batteries, and alkali-metal-ion batteries, such as Li^+, Na^+, K^+ batteries), environmentally friendly bioderived materials, and advanced manufacturing.

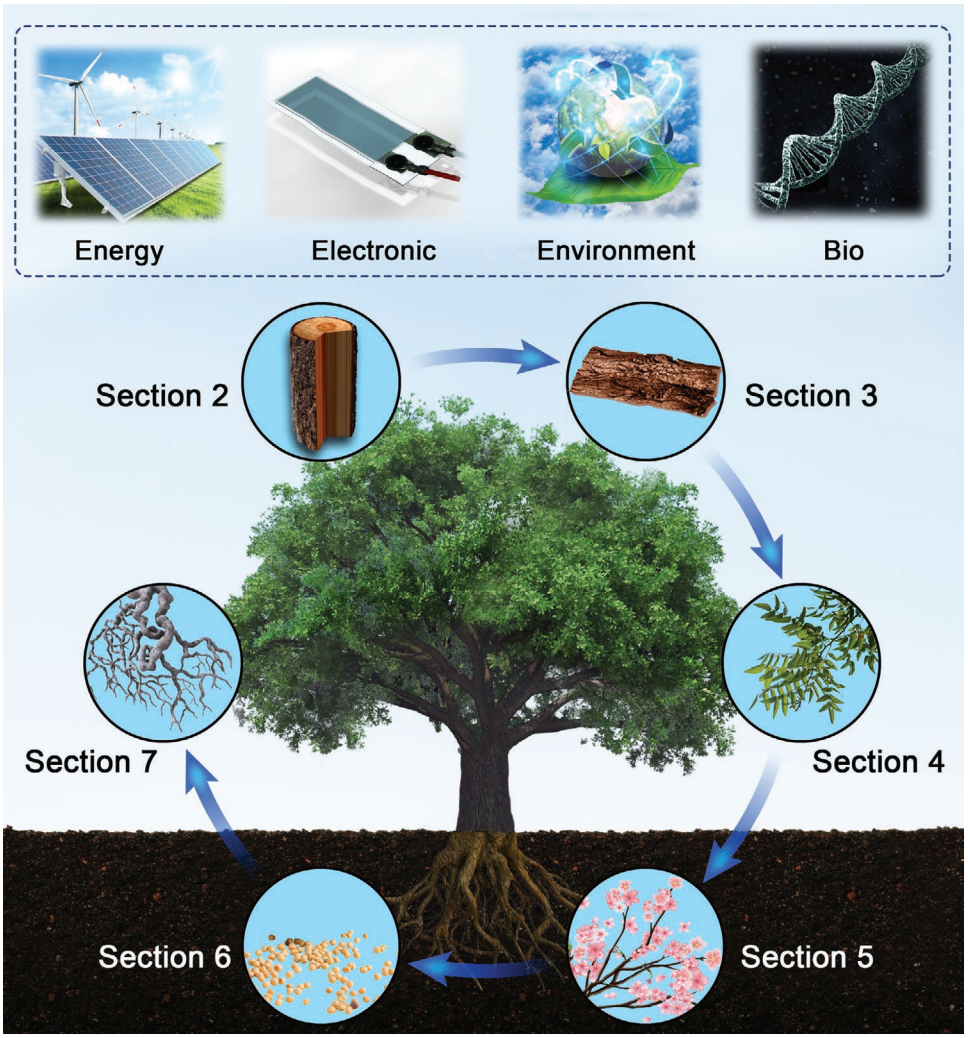

Figure 1. Schematic illustration of the main sections in this review, including materials and structures derived from the trees (trunk, bark, leaf, flower, seed, and root) for the applications in energy, electronic, environmental, and biological fields. The image of the solar cells in the Energy image is reproduced under the terms of the CC-BY Creative Commons Attribution 2.0 Generic license (https://creativecommons.org/licenses/by/2.0/), copyright 2017, user Zak Zak on Flickr (https://www.flickr.com/photos/151836356@N08/34514874094/).

report of functional thin wood was more than a century ago, where the wood was compressed to enhance its mechanical strength.[12] Such thin wood films have been extensively studied again in recent decades for various emerging materials and devices, including electrodes, ion conductors, green electronics, and functional engineering materials.[13,14] These applications are enabled by the inherent physical and chemical characteristics of wood, including the microscale hierarchical pores and aligned channels, anisotropic cell wall fibrils, and hydrogen bonding, which are taken advantage of for further functionalization of the wood. There are two types of wood: softwood and hardwood, which have different nanostructure and microstructure, including the cells types, chemical components, fiber morphologies, and fiber arrangements. The main cells in softwood are tracheid, accounting for 90–95% of the total cells, whilst the main cells in hardwood are fibers and vessel elements, resulting in more complicated structures. In addition, the fibers in softwood are thicker and longer (3–5 mm in length and 20–35 μm in width) than that in hardwood (0.75–1.5 mm in length and ≈20 μm in width). Furthermore, softwood has more organized fiber arrangements in cross section (transverse surface) than hardwood, resulting in a more uniform microstructure.

Most functionalization of thin wood is based on its hierarchical porous structures that form longitudinal channels. Wood has mesopores in the transverse section and nanopores in both radial and tangential sections. All mesopores are formed from the longitudinal wood cells, which also form aligned channels of 0.8–1.6 mm for hardwood and 2–4 mm for softwood along the radial and tangential directions. In addition to mesopores, wood has plentiful nanopores, including pits along the cross-section and ray cells of radial parenchyma. The functions of these pores and channels in tree growth have much inspired the processing of wood into emerging devices. All longitudinal cells in trees function as mass transfer channels for water transport and provide structural support. Similarly, the pits are channels for lateral mass transfer, where fluids are exchanged between

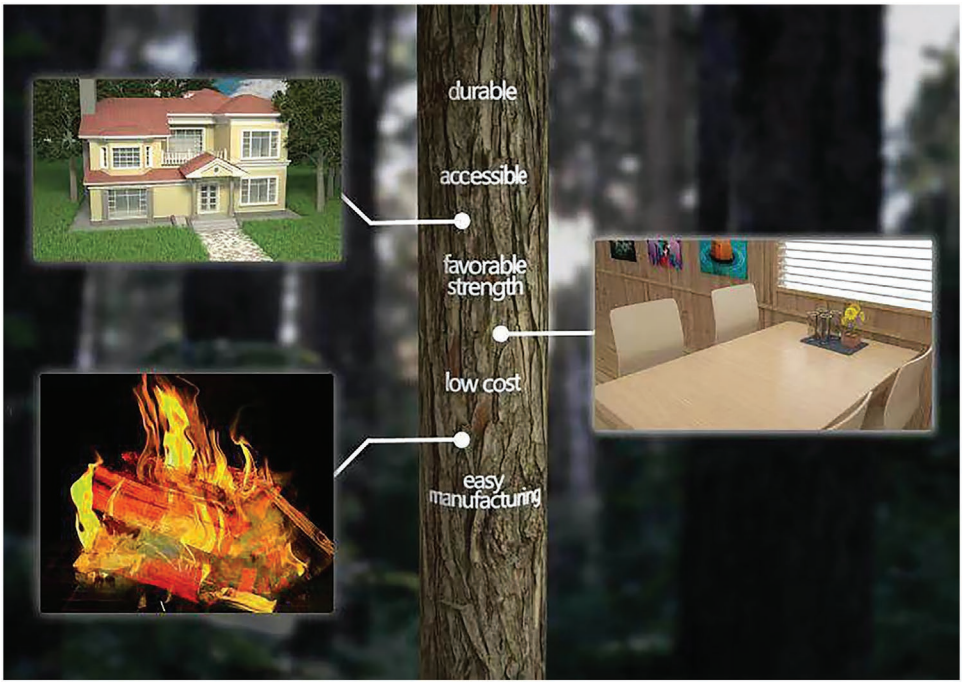

Figure 2. Traditional applications of wood as a bulk engineering material for construction, furniture manufacturing, and combustion.

two adjacent cells for cell-to-cell communication. Analogously, electrode, separator, ion conductor, and desalination devices require hierarchically porous structures and well aligned channels with sufficient surface area for efficient charge and mass transfer. More stimulated to the materials researches, wood cells are elongated in the longitudinal direction and form straight cell channels along the tree stem that can significantly reduce the mass transfer path and enhance transfer efficiency. This property enables wood slices to be used as high-quality ultrathick electrodes with low tortuosity for lithium-oxygen cathode and sodium-metal anode electrodes, as well as for separators with short mass transfer pathways.[15] Despite advances in this field, researchers should further investigate different porous structures and channels derived from different types of wood, scalability, and stability. Due to the significant variations in cell geometries in different tree types, and even the same species grown in different areas, the porous structure and channels could be very different. Therefore, identifying a diverse range of wood with different microstructures suitable for specific applications should be a topic of further study in wood-based materials and device manufacturing.

Another inherent feature of wood that has been explored for advanced materials is its anisotropic fibril alignment. As shown in **Figure 3**a, the cellulose microfibrils in the S2 layer are the main part of the wood cell wall and have a slightly tilted orientation (10°–20°) toward the longitudinal direction, which contributes to the anisotropy of the wood. The nanoscale slots among these cellulose microfibrils are highly anisotropic and suitable channels for external ion transfer. In addition, the chemical modification of cellulose microfibrils by 2,2,6,6-tetramethylpiperidine-1-oxyl (TEMPO)-mediated oxidation converts C6 hydroxyl groups to carboxyl groups, which enhance the surface negative charge of microfibrils and hence changes the surface charge of the mass transfer channel. Therefore, the efficiency of the selective mass transfer can be significantly enhanced.[14]

Significant development in wood-derived functional devices and materials has been achieved. Specifically, functionalization of wood based on its inherent mechanical strength has made process, although the exact mechanism is still unclear. Recently reported super-strong wood fabricated from partial delignification and subsequent thermo-hydrocompression had a specific strength of ≈548.8 MPa.[16] The superior mechanical performance was attributed to the enhanced hydrogen bonding after processing; however, the underlying mechanism has not yet been proven as a phase transition of the remaining lignin and possible changes in bonding between cell-wall polymers also occur. More importantly, even though delignification has been shown to be crucial in enhancing hydrogen bonding after thermo-compression, complete removal of lignin in wood blocks is highly challenging. The uniformity of delignification across the wood block, especially thick wood, is still challenging. Meanwhile, the evaluation of delignification degree should also be further standardized in this field. The pulping process starts with preparation of the raw materials, where the wood is cut into thin chips with a length of 15–20 mm, thickness of 3–5 mm, and width below 20 mm. Reducing the dimensions of the wood chips facilitates penetration of the chemicals, which enhances the delignification process. Delignification is one of the most significant challenges for industrialization of wood blocks for strong engineering materials.

Wood furniture, timber construction, and paper industry are major wood consuming fields. Deforestation can be a severe problem if the rate of harvesting is unbalanced with the speed of cultivation. Promoting the sustainable production and consumption of forest products and sustainable forest management requires some key steps and policy supports. For instance,

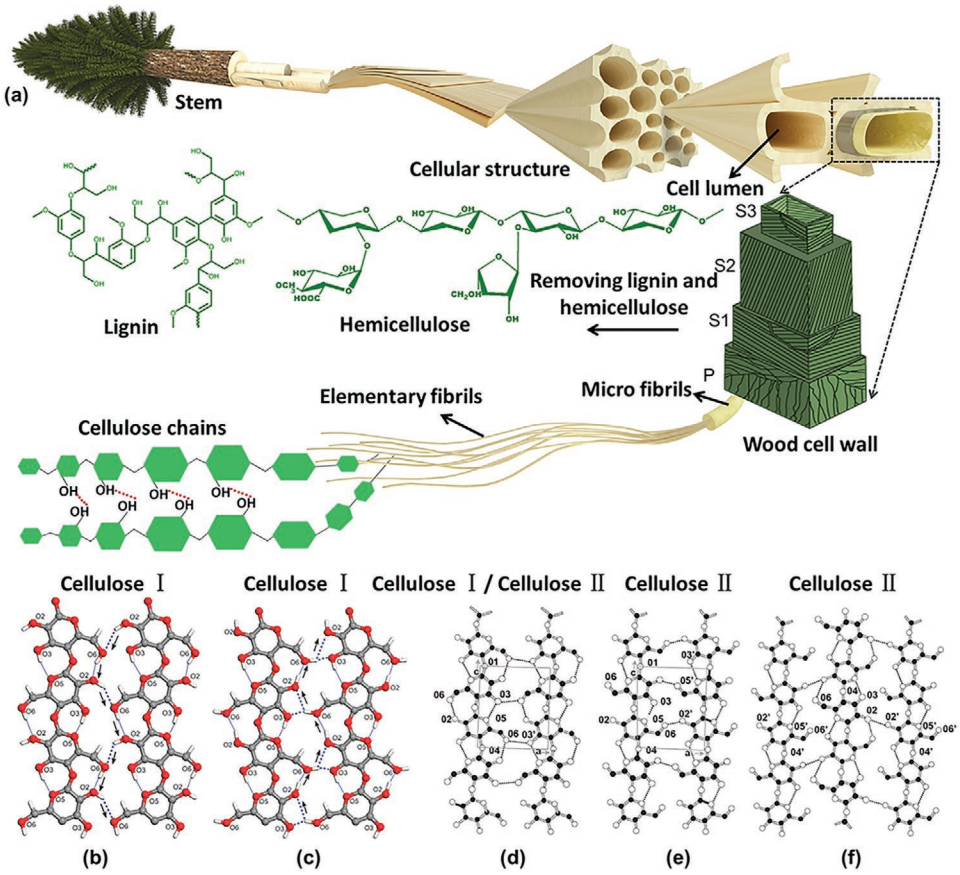

Figure 3. a) Graphical illustration of hierarchical structure of wood, from macroscopic to molecular scale. b,c) Schematics of suggested hydrogen bonding system of cellulose I and cellulose II, $(110)_t$ plane (b) and $(200)_m$ (c) in cellulose I, in which the cellulose chains are linked together by intermolecular hydrogen bonds at O(2)H-O(6). b,c) Reproduced with permission.[11] Copyright 2011, Royal Society of Chemistry. d) 020 plane ("down" chains), e) 020 plane ("up" chains), and f) 110 plane in cellulose II. The hydrogen bonds interaction between cellulose II molecules are stabilized by the O(2)H–O(6) (intra), O(3)H–O(5) (intra), and O(6)H–O(3") (inter) in (d), O(3)H–O(5) (intra), and O(6)H–O(2′) (inter) in (e), and O(2)H–O(6) (intra), O(3)H–O(5) (intra), and O(2)H–O(2′) (inter) in (f). d–f) Reproduced with permission.[20] Copyright 2005, Elsevier B.V.

technological developments aimed at improving the rates of reuse, recycling and bioenergy of wood products, encouraging the development of non-timber products, enforcement in law and forest governance to fight illegal logging and deforestation, and planned reforestation and afforestation.[17] In addition, three sustainability dimensions, including economic, environmental, and social criteria should be considered to balance wood harvesting and cultivation.

2.2. Chemical Compositions of Trunk

The wood cell wall is comprised of the primary wall (P) and secondary wall (S), which account for the bulk of cell wall and can be further divided into three distinct layers, called S1–S3 (Figure 3a). Wood cell wall has a hierarchical structure mainly composed of cellulose microfibrils, which are assembled by 36 chains of cellulose and exhibit different orientation to the tree growth direction (net-like texture in P, 50°–70° in S1, 5°–15° in S2, and 60°–90° in S3); hemicellulose, which presents as a non-crystalline and branched polymer that bind with pectin to microfibrils; and lignin, which is a 3D amorphous phenolic polymer that probably associates closely with hemicellulose by lignin-carbohydrate complex (LCC) through covalent bonds.[18] Many environmentally friendly and sustainable fractionation techniques have been developed in biorefineries to produce high-pure biopolymers. Several excellent reviews have discussed the fundamental properties of the three main components in wood, including the chemistry and structures.[10,19] Some novel and exciting applications of these three components are summarized in this section.

2.2.1. Cellulose-Based Novel Functional Materials and Devices

In 1838, Payen first definitively identified and named cellulose.[21] Approximately 40–50% of the mass of wood is cellulose, depending on the species.[22] Cellulose has a linear long-chain that is comprised of β-D-glucopyranose mono-units connected by β-(1→4)-glycosidic bonds.[23] During the biosynthesis process, van der Waals forces and intermolecular hydrogen bonds promote the parallel accumulation of cellulose chains, forming basic fibrils at the nanoscale, which are further organized into larger fibrils.[24] Cellulose contains both crystalline and amorphous

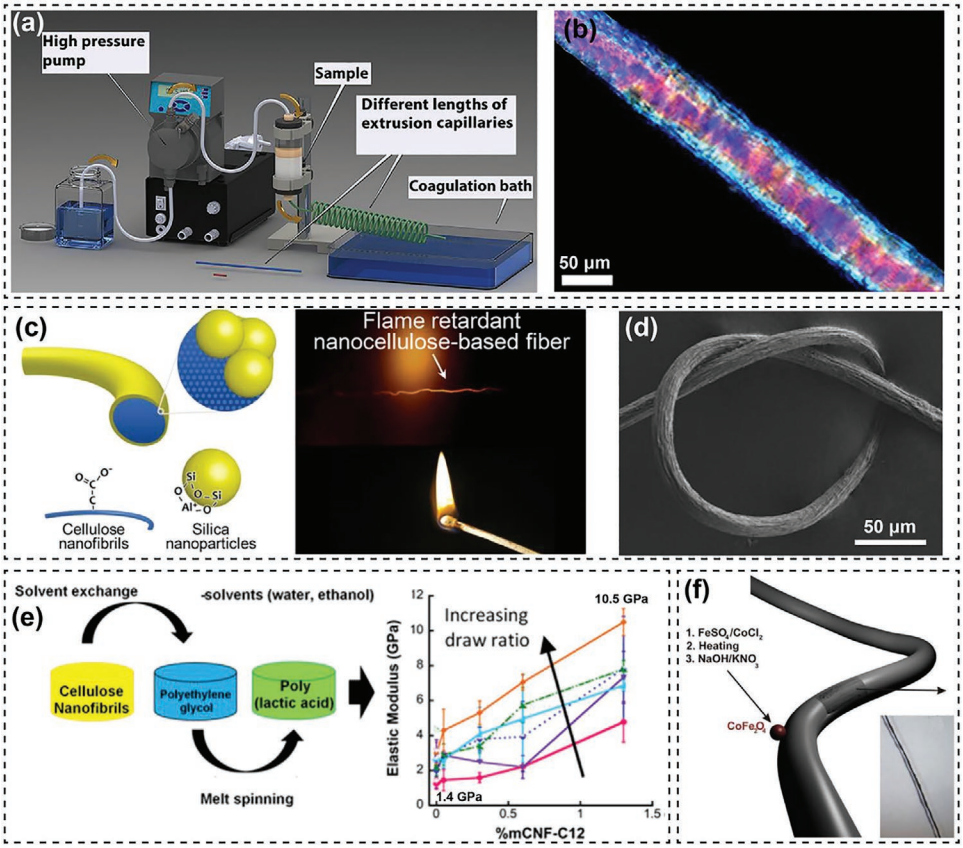

Figure 4. a) Schematic illustration of the preparation of CNF microfibers, and b) the corresponding SEM images. a,b) Reproduced under the terms of the CC-BY Creative Commons Attribution 4.0 International License (https://creativecommons.org/(licenses/by/4.0)).[29] Copyright 2017, The Authors, published by Springer Nature. c) Preparation method and good flame retardancy of CNF/SNP composite fibers, and d) SEM image showing their good flexibility. c,d) Reproduced with permission.[32] Copyright 2017, American Chemical Society. e) Preparation method of CNF/PLA composite fiber and their mechanical performance. Reproduced with permission.[33] Copyright 2018, American Chemical Society. f) Schematic and SEM image of magnetic hybrid fibers. Reproduced with permission.[34] Copyright 2011, Wiley-VCH.

regions in these nanoscale fibrils. In wood, cellulose I, referred to as natural cellulose, is less strongly hydrogen bonded than cellulose II and thermodynamically metastable. Cellulose I is composed of two polymorphs, I_α (a triclinic structure) and I_β (a monoclinic structure). The hydrogen bonding within the I_α and I_β structures is dominated by the O(2)H—O(6) bond, which is the most universal one within the $(110)_t$ and $(200)_m$ planes (Figure 3b,c, respectively).[11] Cellulose II has a more stable crystalline structure than cellulose I and can be produced by redeposition and mercerization.[25] Intrachain and interchain hydrogen bonding in cellulose II model is mainly along the (020) plane for the "down" (center) chains (Figure 3d), (020) plane for the "up" (corner) chains (Figure 3e), and (110) plane (Figure 3f). The cellulose chains are mainly linked by O(2)H-O(6) (intra), O(3)H-O(5) (intra), O(6)H-O(3′) (inter), O(6)H-O(2′) (inter), and O(2)H-O(2′) (inter) hydrogen bonds.[20,26] The nanocellulose obtained by chemical or mechanical treatment of cellulose fibers is classified as cellulose nanofibrils (CNF) and cellulose nanocrystals (CNC).[11] The unique structure of nanocellulose, with its excellent mechanical properties, low thermal expansion coefficient, and high reinforcing potential and transparency, makes them ideal building blocks for smart materials and products. In the following section, we describe nanocellulose-based advanced functional materials, such as 1D fibers, 2D films and papers, and 3D hydrogels and aerogels, which are produced using bottom-up assembly with nanocellulose as the building blocks.

Fibers are extensively used in various industries, such as textiles, wearable electronics, construction, and reinforcing materials, which are subsequently used in many common consumer products.[27] Using natural and biocompatible nanocellulose to produce multifunctional fibers is an increasing trend in recent years. Nanocellulose has been used to prepare mechanically strong fibers; the crystalline cellulose of elementary fibrils has excellent mechanical properties, with a Young's modulus of 110–220 GPa and a tensile strength of 7.5–7.7 GPa.[28] Two main methods for producing 1D cellulose macrofibers from CNF are wet spinning and dry spinning.[18] **Figure 4**a shows the wet spinning method, which are achieved by extruding an aqueous CNF hydrogel into a coagulation solvent, such as ethanol, acetone, dioxane, and tetrahydrofuran. The tensile mechanical properties of individual fibers show high stiffness (≈19–20 GPa) and high toughness (≈28–31 MJ m^{-3}).[29] Figure 4b illustrates that the alignment of the birefringent CNF results in an increase in the birefringence of the fiber, and hence strong colors are observed through imaging fibers between crossed polarizers. In

dry spinning of cellulose macrofibers, a concentrated cellulose nanofiber aqueous suspension is directly spun and then dried in air. The obtained materials have good mechanical properties, e.g., Young's modulus of 12.6 GPa and tensile strength of 222 MPa.[30]

CNF is also an attractive precursor for preparing high-performance carbon fibers with high electrical conductivity. Deng et al. carbonized CNF at a high temperature (2200 °C) and the nanofibers maintained their fibrous morphology after carbonization. No obvious skin–core heterogeneity was observed in their CNF-based carbon fibers, which was attributed to their small size that a constant temperature can be distributed across the fiber during carbonization and incomplete oxidation of the core region during stabilization can be avoided.[31]

Nanocomposite fibers containing nanocellulose have also been demonstrated as advanced functional materials. Nechyporchuk et al. produced flame-retardant macroscopic fibers using CNF and silica nanoparticles (SNP).[32] The addition of SNP promotes the formation of CNF char and improves the thermal flame retardancy of the fibers (Figure 4c). The impressive flexibility of the CNF/SNP fibers is shown in the SEM image in Figure 4d.[32] In addition, nanocellulose was used as a reinforcement agent to improve strength and stiffness of the polymer fiber.[33] CNF and poly(lactic acid) (PLA) composite fibers were obtained by melt spinning. The stiffness of the composite fiber increased by 600% as compared to the pure PLA fiber (from 1.4 to 10.5 GPa; Figure 4e). In addition, functionalized microfibers were obtained by physical dipping and chemical modification, which were transparent and magnetic.[34] $CoFe_2O_4$ particles were synthesized by a simple aqueous coprecipitation reaction between $FeSO_4$ and $CoCl_2$ in the presence of prepared microfibers (Figure 4f). The saturation moment of the modified fibers was up to 6.5 emu g^{-1}, demonstrating the excellent magnetic properties that could be taken advantage of for magnetic shielding, microwave technology, and other applications.

Common paper for printing and art, white cardboard paper, and rice paper, contain cellulose fibers with a diameter of 20–50 μm. These conventional papers are optically opaque due to their roughness and porous structures that produce strong light scattering because of the difference between the refractive index of air (1) and cellulose (1.5).[34] Hence, conventional papers are unsuitable for optoelectronic applications. In addition, the high surface roughness of traditional paper limits its application as an electronic substrate. Optically transparent papers that have higher barrier properties, better visual appearance, and stronger mechanical strength than traditional paper have attracted increasing interest from academia and industries. To produce paper with high optical transmission, physical and/or chemical methods have been used to remove the air within the pores of the paper. This can be achieved by: 1) immersing opaque paper in a material with a similar refractive index, such as oil, resin, and wax; 2) using a cellulose solution; and 3) using deep mechanically treated wood fibers followed by a supercalendering or impregnation process.[35] The light transmittance of some early transparent papers was less than 80%. However, the use of TEMPO-oxidized CNF to prepare transparent nanopaper resulted in a transparency of 90% at 600 nm and a density of 1.45–1.46 g cm^{-3}.[36] The oxidized CNF facilitated densification of the fiber networks, thereby suppressing backward light scattering.

Yano et al. first reported a transparent nanofiber paper similar to glass with high transmittance, high strength, ultralow coefficient of thermal expansion (CTE), and high foldability (**Figure 5**a).[37] Zhu et al. also reported light management of wood cellulose paper and used it in optoelectronics.[38] Figure 5b shows the hierarchical structure of wood microfibers, where each microfiber consists of nanofibers. The transparent paper prepared from the microfibers had both a high transmittance (>90%) and transmittance haze (>90%). In contrast, the total super-clear paper from oxidized CNF had a high transmittance (>90%) but a very low transmittance haze (<1%). This value complies with the standards for high-end displays, which require an optical haze value of less than 1%. The optical haze of super-clear paper (0.5% at 550 nm) is similar to that of flexible glass and lower than that of polyethylene terephthalate (PET). Highly transparent, but hazy paper used for an organic light-emitting diode (OLED) watch effectively reduced glare.[38] In addition, they showed that the transparent nanopaper had good tensile strength, which was higher than that of PET and regenerated cellulose film. In addition, the preparation of the OLED device on a super-clear nanopaper substrate has broadened the application of transparent paper.[38] Another study was flexible transparent electrodes developed by depositing Ag nanowires on a wet nanocellulose sheet, resulting in a high transmittance of 86.5% at 550 nm and a low sheet resistance of 26.2 Ω/sq.[39] This device showed good magnetic and conduction properties (Figure 5c). Furthermore, other functional composite films prepared from nanocellulose and its derivatives have showed great potential in electromagnetic interference (EMI) shielding applications. Zhou et al. developed wearable, flexible electromagnetic interface shielding films with alternating CNF and MXene layers. This CNF/MXene film had high specific shielding effectiveness up to 7029 dB cm^{-2} g^{-1} due to the high impedance mismatch and interaction between EM and high-density electron carriers when EM radiation passes through the CNF/MXene films (Figure 5d).[40] Wang et al. developed superhydrophobic shape-memory adhesive films by adhering a layer of superhydrophobic polyurethane (PU) onto a PU-CNF substrate to obtain the hair-like skin structure (Figure 5e).[41] This smart film has great potential in many applications, such as microreactions, biodetection, and fluidic devices.

In addition to the abovementioned applications, CNF-based composite membrane has been widely used in selective gas-separation. Membranes fabricated by uniting inorganic metal–organic frameworks (MOFs) with traditional polymers encounter poor polymer-MOF affinity, which results in interfacial defects and gas leakage in the gas-separation applications. To address this issue, Matsumoto et al. reported an ultraselective gas separation that was enabled by an nanoporous MOF embedded gas-barrier CNF film.[42] ZIF-90 MOFs (ZIF = zeolitic imidazolate framework) reacted with the carboxyl group of CNF to form tight contact for gas separation. The obtained ZIF-90/CNF composite film illustrated extremely high flux of CO_2 (2.97×10^3 gas permeance units (GPU)) and high selectivity (CO_2/CH_4 = 123) for selectively separation of CO_2 from a CO_2/CH_4. In another study, Zhang et al. developed a gas-separation membrane by using UiO-66-NH_2 (Zr-based MOF) nanoparticles and CNF-COOH.[43] Attributed to the electrostatic forces and acid-base interaction between the −COOH groups of CNF and

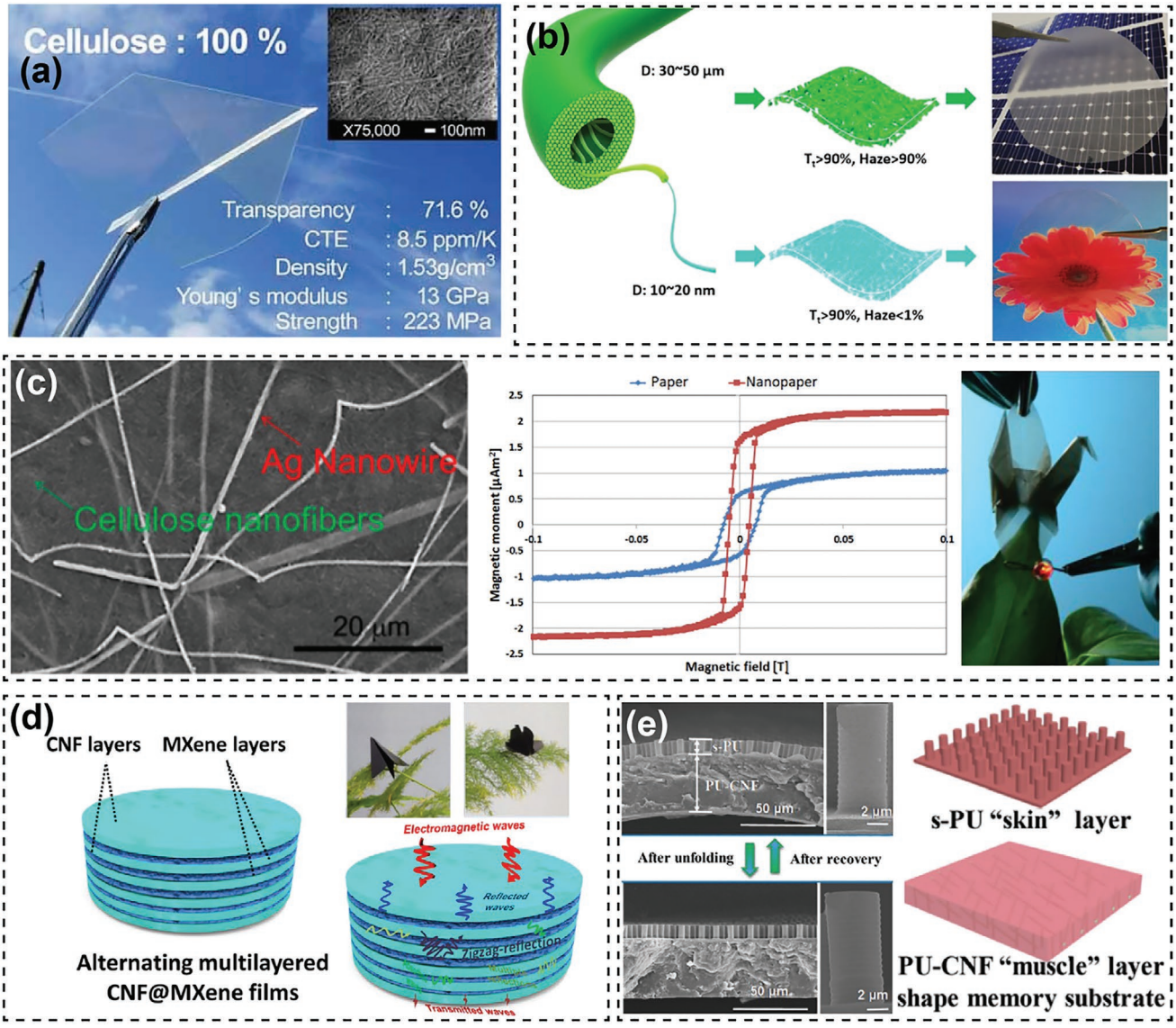

Figure 5. a) Photograph of high-quality transparent paper. Reproduced with permission.[37] Copyright 2009, Wiley-VCH. b) Schematic of the preparation of transparent paper from wood. Reproduced with permission.[38] Copyright 2016, American Chemical Society. c) SEM image of CNF-based film, its magnetic properties, and photograph of illuminating the conductive film. Reproduced with permission.[39] Copyright 2016, American Chemical Society. d) Schematic of the preparation of CNF/MXene films and EM shielding mechanism, (inset) photographs of the flexible film. Reproduced with permission.[40] Copyright 2020, American Chemical Society. e) SEM images of shape-memory adhesive film before and after recovery, and schematics of the design strategy of the film. Reproduced with permission.[41] Copyright 2019, Royal Society of Chemistry.

the $-NH_2$ groups of MOF, the CNF and MOF can be easily anchored together. The composite membrane displayed ideal interfacial morphology that the UiO-66-NH_2 is well-dispersed in the CNF matrix. The porous structure of UiO-66-NH_2/CNF membrane strengthened the diffusion of CO_2 molecules and improved CO_2 separation performance, which showed that CO_2 permeability reach 139 Barrer and the CO_2/N_2 selectivity ratio is as high as 46.

In addition to CNF, CNC has been largely developed to prepare functional 2D films. To prepare CNC, the natural cellulose extracted from trees is acid hydrolyzed to selectively remove amorphous regions of cellulose microfibers, leaving crystalline nanorods in the reaction solution (**Figure 6**a).[44] Figure 6b shows a schematic diagram of a chiral nematic structure in a CNC film after different acid treatments, where P/2 is the half-spiral pitch. Since P/2 is at a similar scale to the wavelengths of visible light, the CNC film appears iridescent. Cheng et al. also reported the correlation between electrostatic interactions and the chiral nematic structures of CNC. The variations in P/2 values produced after different acid treatments resulted in the generation of different colors.[45] It was found that the CNCs formed a chiral nematic structure by electrostatic repulsion as a consequence of the negative surface charge.[45] This change can be detected by circular dichroism (CD) and UV–vis spectroscopy, which may provide guidance for developing new sensors. Moreover, free-standing chiral plasmonic composite

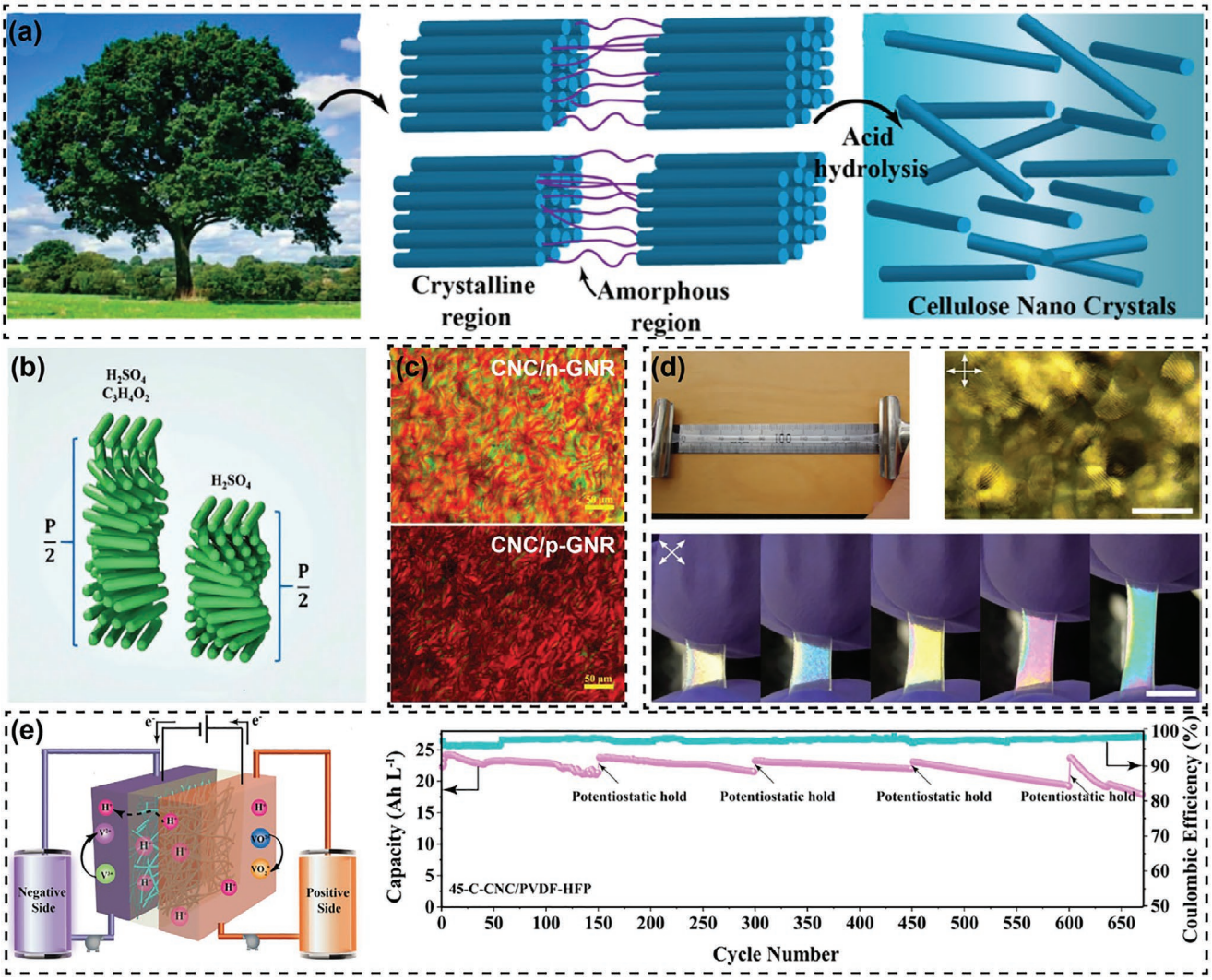

Figure 6. a) Schematic illustration of CNC preparation using acid hydrolysis. Reproduced with permission.[44] Copyright 2019, American Chemical Society. b) Schematic diagram of the half-helical pitch (P/2) change of CNC treated with different acids. Reproduced with permission.[45] Copyright 2019, Wiley-VCH. c) Images of CNC/n-GNR hybrid films and CNC/p-GNR hybrid films ("n" represents negative charge, "p" represents positive charge). Reproduced with permission.[46] Copyright 2019, Wiley-VCH. d) Photographs of CNC-based films during stretching under polarized light. The film changes color under stretching. Reproduced under the terms of the CC-BY Creative Commons Attribution 4.0 International License (https://creativecommons.org/licenses/by/4.0).[47] Copyright 2019, The Authors, published by Springer Nature. e) Schematic illustration of a flow battery using the CNC/PVDF-HFP membrane, and its cycle stability shown by the CE and discharge capacity of the membrane at 100 mA cm^{-2}. Reproduced with permission.[44] Copyright 2019, American Chemical Society.

films were designed by coassembling anisotropic plasmonic gold nanorods (GNRs) and rod-like CNCs.[46] The effects of surface charge and the concentration of the GNRs on the structure and optical properties of the CNC/GNR films were systematically examined. The CNC/GNR hybrid films retained the photonic characteristic of the CNCs host while concomitantly possessed the plasmonic resonance of GNRs. The chiral plasmonic hybrid films showed tunable plasmatic optical properties, e.g., controlling the color of the film by modifying the zeta potential of CNF/GNR hybrid films by adding different content of gold nanorods (Figure 6c).[46] Another study fabricated CNC-based stimuli-responsive stretchable optics by mixing CNCs with an elastomer.[47] Vivid colors appeared when the film was stretched and disappeared when the elastomer returned to its original shape (Figure 6d). Furthermore, Mukhopadhyay et al. prepared CNC-based ion-selective membranes for flow battery applications.[44] The proton-conductive CNC was incorporated in a matrix of semicrystalline hydrophobic poly(vinylidene fluoride) hexafluoropropylene (PVDF-HFP) and used to produce a stable and highly ion-selective membrane. The Coulombic efficiency (CE) of this device was 98.2%, and performed at a current density of 100 mA cm^{-2} over 650 cycles (Figure 6e). The use of CNC-based membranes in flow batteries is expected to contribute to the development of low-cost energy storage technology.

In addition to 1D and 2D materials, nanocellulose can be assembled into 3D composites and aerogels, which have shown promising properties such as low density, low thermal conductivity, high specific surface area, and accessible surface

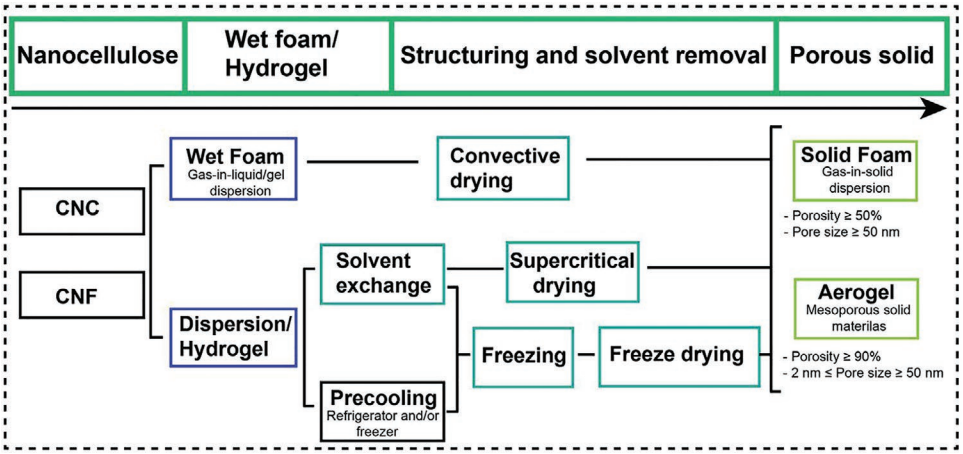

Figure 7. Schematic illustration of processes used to form nanocellulose-based foams and aerogels.

chemistry.[48] In this review, we define a nanocellulose-based foam as a heterogeneous porous material with a porosity higher than 50% and a pore size greater than 50 nm. In contrast, we define a nanocellulose-based aerogel as a particular nanocellulose-based foam with a high porosity (>90%) and a pore size in range of 2–50 nm. There are two main steps to produce nanocellulose-based aerogels (**Figure 7**). A wet foam or hydrogel is prepared from dispersion first, which is followed by the removal of the solvent by evaporation (oven drying), supercritical drying, or freeze drying preceded by solvent exchange. In addition, the foams can be structured from the dispersion by freeze-drying the solvent.[49]

Nanocellulose foams and aerogels have various significant properties. First, ultralight and highly porous nanocellulose-based foams and aerogels have a density of 1–200 kg m^{-3}, with a corresponding porosity >99%.[50] **Figure 8**a shows a cellulose aerogel with an ultralow density (1 mg cm^{-3}) and ultrahigh porosity (99.9%) that was produced using a freeze-drying method with a cellulose nanofibril hydrogel. An aerogel with a porous structure was formed due to widespread hydrogen bonding between the cellulose nanofibrils.[51] Second, the high specific surface area of the foams is ideal for applications such as insulators, electrodes, and adsorbents.[52] In addition, good controllability of the pore size and morphology can be achieved by adjusting the processing route, particle size, shape, and interactions. Another benefit of these materials is their superior mechanical properties. Figure 8b shows the compressive stress–strain curves of CNF aerogels with different densities.[51] These curves have three main stages: i) linear elastic behavior caused by bending of the cell wall; ii) a plateau area indicating plastic deformation due to collapse of the cell; iii) densification regime, where opposing cell walls approach each other and eventually contact.[49,51] Finally, aerogels and foams have low dielectric loss, low thermal conductivity, and good absorption of sound. These properties make nanocellulose foams and aerogels of interest for a wide range of applications, including fire retardant and thermal insulation materials, devices for energy storage, and scaffolds for pharmaceutical and biomedical applications.

This section summarizes recent advances in these fields. Nanocellulose-based foams and aerogels have thermal conductivity (k) values below 25 mW m^{-1} K^{-1}, similar to that of air, which makes them super-insulating materials.[53] Wicklein et al. developed anisotropic composite foams by combining nanocellulose, graphene oxide, and sepiolite, which had excellent thermal conductivity (15 mW m^{-1} K^{-1}) and fire retardancy; they proposed that these materials could replace commercial expanded polystyrene (EPS) foams ($\lambda = 35$ mW m^{-1} K^{-1}) (Figure 8c).[54] In another study, thermally insulating aerogels were fabricated using CNF and metallic MoS_2, which showed highly desirable thermal and combustion properties (k = 28.09 mW m^{-1} K^{-1}; limiting oxygen index of 34.7%).[55] Vertical combustion tests also highlighted excellent flame retardancy and self-extinguishing ability of the aerogels (Figure 8d). Nanocellulose foams and aerogels have also been used in energy storage systems, but their electrical conductivity is usually lacking. Cao et al. used nanocellulose as a printing additive and stable scaffold in 3D printing of lithium metal battery.[56] The dried CNF/$LiFePO_4$ electrode printed with different layers is shown in Figure 8e. Nanocellulose has good conductivity after carbonization, and does not require other conductive additives. The printed electrode showed good ionic accessibility and excellent cycle stability over 300 h (Figure 8e). Porous lithium metal electrodes prepared with nanocellulose efficiently inhibited the formation of lithium dendrites. In addition, nanocellulose aerogels and foams have been applied in the biomedical and pharmaceutical fields as scaffolds and templates, which have been shown to support cell growth and proliferation. Cell culture using CNF aerogel scaffolds resulted in less than 5% cell death during 72 h of cell growth.[57] Another study used hydroxyapatite nanocrystals to mineralize cellulose hydrogels, where the precursor minerals penetrated the nanopores of the aligned CNF network. The ultrastructure and mechanical properties of the obtained mineralized gel were strikingly similar to those of bone and dentin (Figure 8f).[58]

2.2.2. Hemicellulose-Based Novel Functional Materials and Devices

Hemicellulose is a heteropolysaccharide that accounts for about 15–35% of the mass of wood cells.[59] Unlike cellulose that are linear and chemically homogenous, hemicellulose is highly branched polysaccharide that consists of xylose, glucose, arabinose, galactose, mannose, and galacturonic acid.

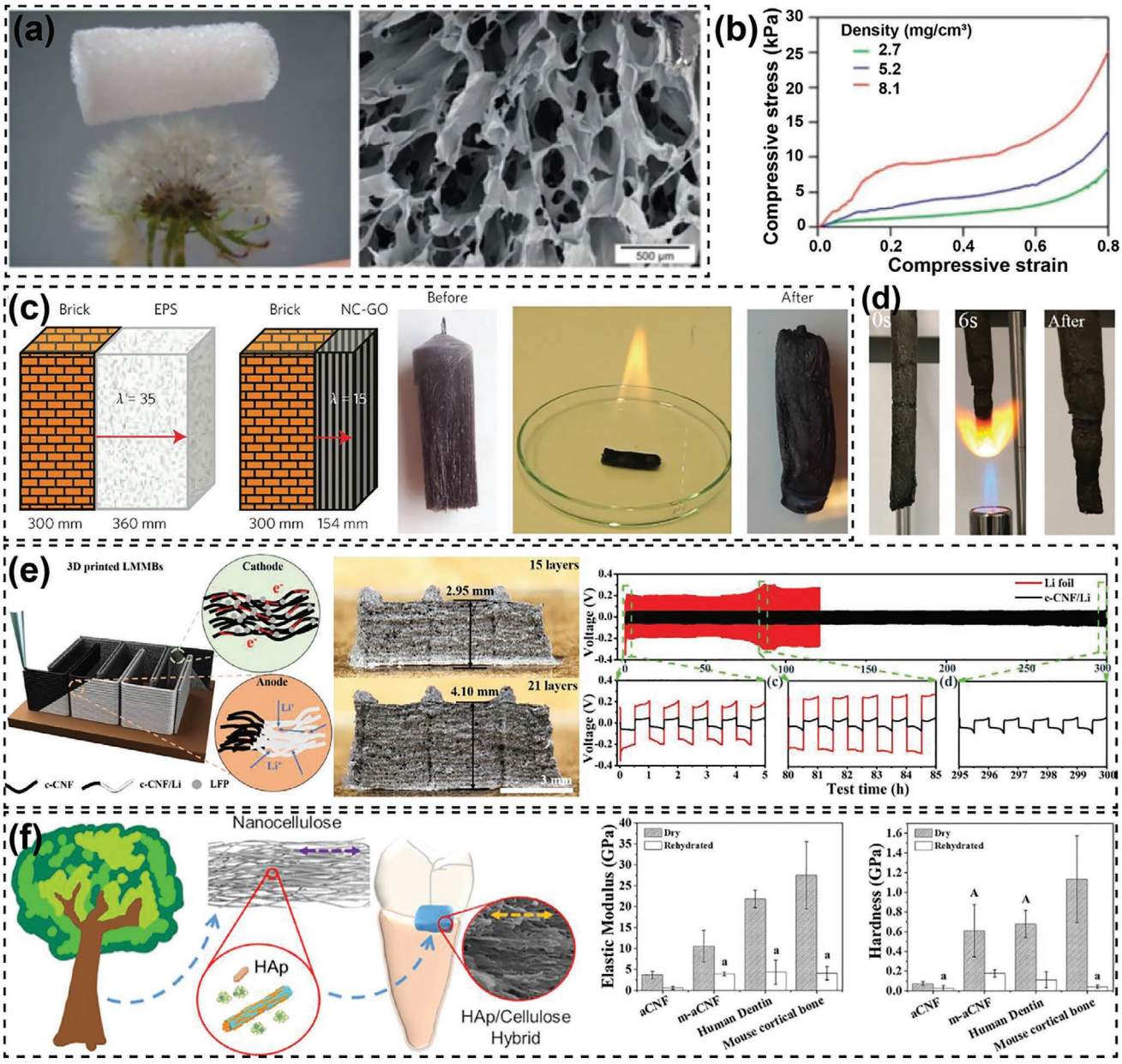

Figure 8. a) Photograph of CNF aerogel on top of a dandelion and SEM image of its porous structure. b) Compressive stress–strain curves of aerogels with different densities. a,b) Reproduced with permission.[51] Copyright 2014, Royal Society of Chemistry. c) Schematic comparison of the thickness of polystyrene and nanocomposite foam needed for house insulation, and the burning performance of the aerogel. Reproduced with permission.[54] Copyright 2014, Springer Nature. d) Vertical burning test of the CNF/MoS_2 aerogel. Reproduced with permission.[55] Copyright 2017, Royal Society of Chemistry. e) From left to right are schematics of 3D-printed lithium metal batteries as a scaffold to host Li, photographs of printed electrode with different layers, and cycle performance of the cell at a current density of 5 mA cm^{-2}. Reproduced with permission.[56] Copyright 2019, Wiley-VCH. f) Schematics of nanocellulose-based gel used in human hard tissues and its corresponding mechanical properties compared to other biomaterials. Reproduced with permission.[58] Copyright 2019, American Chemical Society.

Different woods have different hemicellulose compositions, structures, and concentrations. In hardwoods, the major component is *O*-acetyl-4-*O*-methylglucuronoxylan, in which one-tenth of the xylopyranose backbone units are substituted at C-2 with (1→2)-linked 4-*O*-methyl glucuronic acid residues.[60] In contrast, the major hemicellulose in softwood is *O*-acetyl-galactoglucomannan, which has a backbone connected mannose and glucose units by β-(1→4)-glycosidic bonds with the branched galactose units linked to the mannose and glucose by α-(1→6)-glycosidic bonds.[60] Various processing technologies, including alkaline extraction,[61] dilute acid pretreatment,[62] liquid hot water extraction,[63] microwave treatment,[64] steam treatment,[65] and ionic liquid extraction,[66] have been developed to extract hemicellulose from wood. However, some key issues, such as reducing hydrophilicity and increasing thermal stability and mechanical flexibility, should be addressed to facilitate

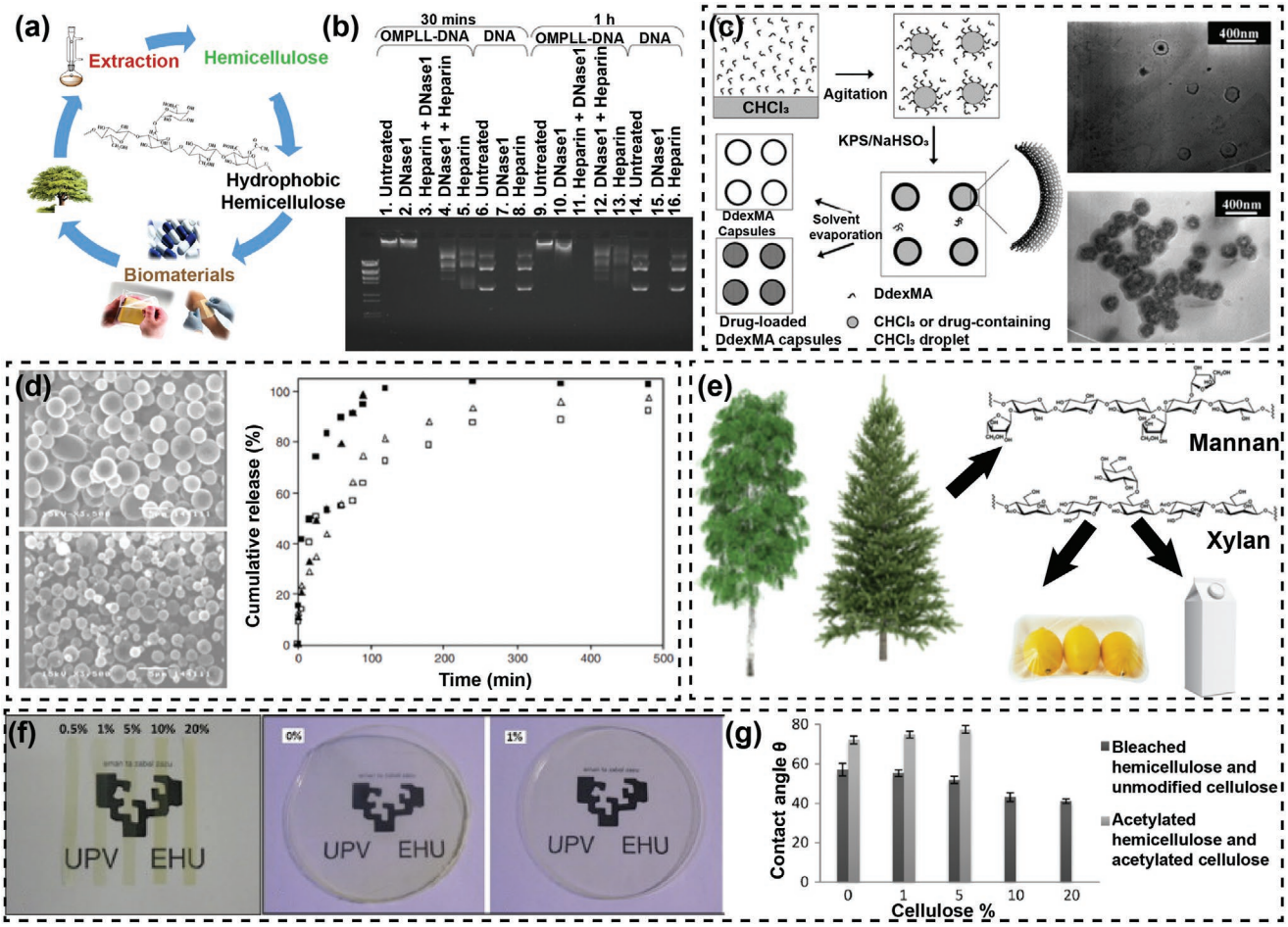

Figure 9. a) Schematic diagram of the process for extracting hemicellulose and applying it to the biomedical field. Reproduced with permission.[60] Copyright 2017, Wiley-VCH. b) Treated DNA complex results from 0.6% agarose gel electrophoresis analysis. Reproduced with permission.[75] Copyright 2009, Elsevier B.V. c) Schematic illustration of the process for preparing polysaccharide nanocapsules and the corresponding SEM images. Reproduced with permission.[81] Copyright 2006, Elsevier B.V. d) SEM images of galactoglucomannan-based microspheres and their release properties. Reproduced with permission.[80] Copyright 2008, Sage Publications Ltd. e) Hemicellulose-based polysaccharide from trees, which showed good potential in food-packaging applications. Reproduced with permission.[82] Copyright 2012, Elsevier B.V. f) Optical microscopy images of hemicellulose-based hydrophilic films. g) Contact angles of the composite films shown in (f). f,g) Reproduced with permission.[83] Copyright 2014, Elsevier B.V.

advanced production. Recently, native hemicellulose materials have been modified to synthesize new hemicellulose derivatives, for example, using esterification,[67] acetylation,[68] oleoylation,[69] fluorination,[70] etherification,[71] and crosslinking,[72] to meet the demands of functional applications. The following sections describe the use of such hemicelluloses for various applications.

Biomedical Applications: Hemicellulose-derived materials have been extensively studied in recent years to guide the design and manufacture of biomedical materials. Hydrophobization and crosslinking have been used to modify hemicellulose (**Figure 9**a). In comparison with unmodified hemicellulose, the modified hemicellulose is a suitable precursor for producing water-resistant materials toward biomedical applications. Several types of hemicellulose have been successfully used to inhibit the growth of different tumors by inducing the activity of the host's immune system.[73] A study showed that oxidized mannan as a biologically active substance can be combined with a vaccine (MUC) to obtain a fusion protein (M-FP), which could be used as a target for cancer immunotherapy.[74] Apostolopoulos et al. reported that oxidized mannan poly-L-lysine (OMPLL) and reduced mannan poly-L-lysine (RMPLL) could be used to target DNA vaccines to antigen-presenting cells (Figure 9b).[75] In addition, hemicellulose has antimicrobial activity. When microorganisms cause infectious diseases by attacking host cells and tissues, good adhesion is essential to allow pathogens to obtain nutrients and deliver toxic substances into the cells of host tissues.[76] Iwamoto et al. reported that mannan inhibits the adhesion of several *Candida albicans* strains to plastic plates, therefore coating medical devices with mannan-type hemicellulose can reduce *C. albicans* adhesion.[77]

Hemicellulose has also been widely used in wound dressings. The ideal wound dressing should maintain a high humidity environment at the wound dressing interface, remove exudates, allow gas and vapor exchange, be impermeable to microorganisms and water, can reduce pain caused by the wound, and can be removed without damaging the healing wound.[78] A hemicellulose-based wound dressing (Veloderm) has been commercialized by Medestea Research & Production, Italy. Veloderm is a biofilm

with a polymeric structure consisting of hemicellulose microfibers that has been described by the manufacturer as a wound dressing that provides selective penetration of gas and vapor as well as prevents water and microorganisms from the penetration, which thus protects the wound from dirt and bacteria penetrating from the outside. Veloderm was also claimed to reduce pain and create an environment for granulation and re-epithelialization, which promotes rapid and optimal wound healing.

In recent years, interest in hemicellulose-derived biopolymers as a drug-delivery system has greatly increased. Xylan is known to be degraded by xylanases and β-xylo-sidases secreted by the human colonic microflora.[79] The presence of microorganisms that secrete these enzymes in the colon affect the use of hemicellulose as a drug-carrier polymer for colon-specific drug delivery. Several forms of drug-delivery systems, including nanoparticles, microparticles (microcapsules and microspheres), and nanocrystals, have been reported.[80,81] Jiang et al. prepared crosslinked polysaccharide nanocapsules by polymerization of methacrylated *N,N*-diethylaminoethyl dextran (DdexMA) and DdexMA-vinyl terminated polylactide macromonomers (PLAM) (Figure 9c). The loaded drug can be released again in a manner that lasts up to 100 h.[81] Edlund et al. fabricated galactoglucomannan (GGM)-based microspheres as a drug-delivery system, which contained caffeine (a very small hydrophilic substance) and macromolecular model protein (bovine serum albumin). The release rate of GGM-based microspheres varied depending on several factors such as pH, the type of encapsulating substance (Figure 9d).[80]

Packaging and Other Applications: Xylans and mannans as the main hemicelluloses in wood cell walls can potentially be recovered in large quantities from biorefineries. Xylan and mannan have good film-forming ability and biodegradability, making them effective substitutes for the petroleum-based materials currently used for food packaging (Figure 9e).[82] The development of xylan and mannan-based films and coatings as sustainable packaging materials has received widespread industrial attention. A key patent for hemicellulose membranes was reported by Xylophane, Sweden, in 2008.[84] Since then, the number of academic publications on the subject has grown steadily. The main disadvantage of polysaccharide films is usually their sensitivity to moisture.[85] Recently, a patent owned by Xylophane has proposed a method for producing flexible films and coatings for packaging based on hemicellulose by using a crosslinking or hydrophobic agent, which provides a barrier to oxygen, aromas, and/or grease and has improved moisture resistance.[85] In the work of Gordobil et al., xylan-cellulose films in different proportions were prepared by solvent casting (Figure 9f).[83] Acetylated hemicellulose served as the hydrophobic matrix and acetylated cellulose were used to increase the hydrophobicity of the film. The contact angle of the film increased from 57° to 72°, which increased the hydrophobicity of the film (Figure 9g). Péroval et al. developed an arabinoxylan film grafted with omega-3 fatty acid to improve its water resistance. The contact angle of the film increased from 66.8° to 115° after grafting.[86] In another study,[87] hemicellulose acetate was used as an internal plasticizer for a cellulose acetate film. The cellulose acetate films with 5% xylan acetate had a tensile strength of 40 MPa, while the films without xylan acetate even cannot be cut into unnotched specimens for mechanical testing.

In addition, hemicellulose has been widely used in coating applied in the pulping and paper-making industry. Coatings play a key role in improving paper quality, e.g., decreasing ink absorption. Coated paper provides clearer and glossier printing results, and water and grease resistance in packaging applications. In the food industry, coatings can be used as moisture barriers to prevent food spoilage. Kisonen et al. developed O-acetyl galactoglucomannan (GGM) esters for barrier coatings used in food packaging.[88] A layer of GGM esters can be effectively coated on rough inorganic layer of cardboard. The penetration of the grease barrier of a GGM-coated carton was controlled by adjusting the GGM content. Hence, this review has demonstrated that hemicellulose-derived materials have been widely used in many applications, where further investigation would benefit this developing area.

2.2.3. Lignin-Based Advanced Functional Materials and Devices

Cellulose and hemicellulose have been widely used for the production of paper, biofuels, and sugars in both the paper industry and lignocellulosic biorefineries. Lignin is the major byproduct from these industries, which has not yet been effectively utilized. The lignin content in wood is in the range of 15–30 wt%, where softwood has a higher lignin content than hardwood, which can be up to 30 wt%.[1,89] The majority of the lignin produced in the paper industry (>95%) is burned to generate heat and electricity, while less than 2% is recovered for use as dispersants, adhesives, additives, and surfactants for concrete.[90] Lignin is a complex and water-insoluble amorphous polymer with plentiful aromatic moieties, which is biosynthesized from three main monolignols of *p*-coumaryl, coniferyl, and syringyl alcohols by forming condensed carbon—carbon bonds and uncondense ether bonds. The inherent characteristics of lignin, such as its high carbon content, high aromaticity, various functional groups, antioxidant ability, UV absorbance, biocompatibility, and abundance offer great potential for making high-value products.[91] Three main methods have been used to produce lignin-based materials (**Figure 10**): 1) lignin as a biopolymer component in thermoplastic polymer blends; 2) improving the interfacial properties of lignin by chemical modification and grafting that provides better compatibility with synthetic polymers; and 3) depolymerizing lignin into platform chemicals that can be converted into monomers for some polymer syntheses.[92] The large number of published reviews on different lignin applications indicate the great interest in such lignin-based polymers.[90,92–94] This section provides an overview of the latest research on converting lignin into high-value materials for energy storage, biomedical, and adsorption applications.

Rechargeable Batteries: In recent years, renewable and clean energy storage systems have been significantly sought after as a replacement for traditional fossil fuels. To meet the growing demand for large-scale applications, such as electric stationary energy storage grids and vehicles, many studies have investigated the electrochemical performance of each component in rechargeable batteries, such as the cathode, anode, binders, and electrolyte.[91] In addition, the cost of the processing method is especially critical for large-scale applications. This section provides an

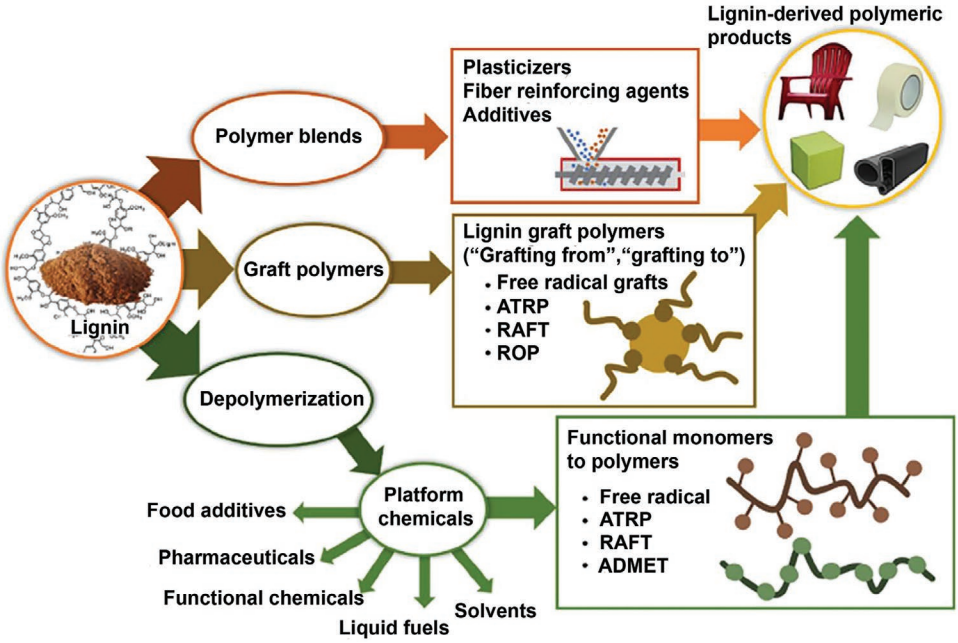

Figure 10. Schematic illustration of the strategies for producing value-added polymeric materials from lignin. Reproduced with permission.[92] Copyright 2019, Elsevier B.V.

overview of lignin as a low-cost and renewable biomass material in recent advanced rechargeable battery applications, such as lithium batteries, sodium batteries, and flow batteries.

Cao et al. developed a Li metal anode using lignin-derived 3D scaffolds for lithium dendrite suppression.[95] They used a boron nitride (BN) sheet grafted with sodium lignosulfonate by carbonization to obtain a layered structure (**Figure 11**a). The addition of the thermally conductive BN increased heat dissipation and charge transfer in the porous and layered structures, thereby stabilizing the lithium metal anodes. The electrode maintained good stability after several charge and discharge cycles, and also effectively suppressed the growth of lithium dendrites. Gong et al. first reported a lignin-based gel polymer electrolyte (GPE) to achieve green and environmentally friendly lithium batteries.[96] Lu et al. used lignin as a binding material for both the positive ($LiFePO_4$) and the negative electrode materials (graphite), which displayed relatively good stability and high specific capacity of the battery.[97]

Due to the potential low cost and the abundance of the sodium resources, sodium battery is considered as a promising alternative to lithium battery. Recently, hard carbon with a layered pore structure and an increased interlayer lattice distance was reported to be advantageous for the storage and transportation of Na^+ ions. As a precursor for hard carbon, lignin-based hard carbon anodes have been used for sodium batteries. Du et al. studied an N-doped lignin porous carbon structure by adding SiO_2 nanoparticles to the precursor and etched it after pyrolysis in N_2.[98] The battery showed high reversible capacity of 100 mAh g^{-1} after 1100 cycles (Figure 11b).

In addition, lignin has been used in flow batteries. Mukhopadhyay et al. first used an ultrafiltered lignosulfonate as the electrolyte of an aqueous flow battery.[99] Quinone analogs in lignosulfonate can undergo redox reactions for energy storage. Figure 10c shows the cyclic voltammetry curve of lignin on the carbon paper working electrode without any substantial signs of irreversibility. The measured current density of the flow cell was up to 20 mA cm^{-2} (Figure 11c). However, there are few phenolic polymers that can convert phenol into quinone from traditional lignin, which contains monomer structures mostly composed of G-lignin, H-lignin, and S-lignin. This two-electron redox reaction can be achieved in catechyl lignin (C-lignin), but the content of C-lignin in traditional lignin is small.[100] C-lignin was found in cacti of one genus (Melocactus), in the seed coating of the vanilla orchid and candlenut (*Aleurite moluccanus*) shells.[100]

Supercapacitors: Supercapacitors are widely used in electric vehicles and other devices due to their long cycle life (>10^5 cycles), high power density, and wide operating temperature range (–40 to 80 °C).[101] Energy storage in supercapacitors is mainly achieved by electrostatic adsorption of ions on the electrode–electrolyte interface and faradaic reaction of active materials. Various electrode materials have been developed for supercapacitors in recent years.[102] Among them, porous carbon-based materials have received tremendous attentions due to their superior electrical conductivity, high specific surface area, and high chemical stability. Lignin is an ideal carbon precursor for porous carbon electrodes. In addition, the redox reaction with lignin as a result of the phenol structure provides pseudocapacitance. Milczarek et al. first reported that phenol moieties in lignin can be used for electron storage and exchange during redox cycling.[103] Figure 11d shows a simplified presentation of electrochemical redox reactions of phenol functional groups in a lignosulfonate biopolymer in a polypyrrole matrix. Jeon et al. developed a lignin-derived nanoporous carbon electrode material for supercapacitors (Figure 11e).[104] Carbonized lignin has excellent charge-storage capacity and good capacity

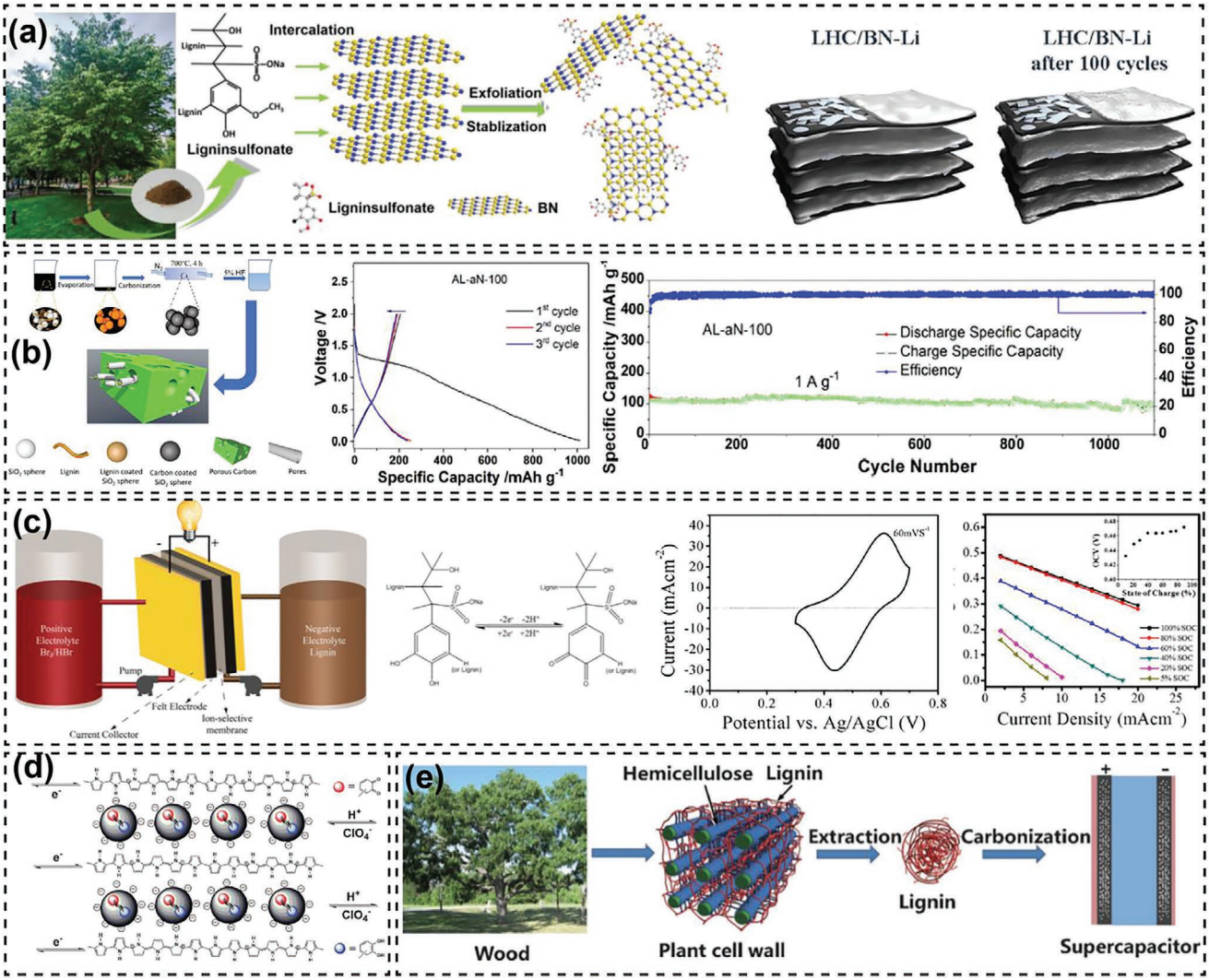

Figure 11. a) Schematic of the preparation method for lignin-based scaffolds for Li battery applications, and the corresponding Li deposition behavior before and after cycling. Reproduced with permission.[95] Copyright 2019, Wiley-VCH. b) Schematic illustration of synthesis of the process for preparing lignin-based Na anodes and their Na battery performance. Reproduced with permission.[98] Copyright 2019, IOP Publishing, Ltd. c) Schematic of the lignin flow cell assembly process, the redox reaction involving lignin molecules, and the cell performance. Reproduced with permission.[99] Copyright 2018, American Chemical Society. d) Redox reaction involving quinone functional groups in lignin. Reproduced with permission.[103] Copyright 2012, American Association for the Advancement of Science. e) Schematic of lignin being carbonized to prepare supercapacitor electrodes. Reproduced with permission.[104] Copyright 2015, Wiley-VCH.

retention. Additionally, lignin can be used as a carbon source via templating to obtain hierarchical porous carbon. This supercapacitor with lignin-based templated carbon electrodes showed high energy density and excellent cycling performance.

Biomedical Applications: Lignin-based nanomaterials can overcome the limitations of lignin, e.g., complex macromolecular structure, high polydispersity, immiscibility with host polymer matrices, and provide morphological and structural control of lignin to improve blending properties with the host matrix.[105,106] The preparation of nanostructured lignin also provides the possibility of using lignin-based materials for high-value biomedical applications, such as drug/gene delivery and tissue engineering.[107] Recently, lignin has been used to develop various nanomaterials, such as nanotubes, nanofibers, and nanoparticles.[106,108] Lignin nanoparticles (LNPs) are widely used in biomedical fields due to key advantages such as improved polymer blend performance and higher antioxidant activity due to the high specific surface area.[109] Furthermore, LNPs possess active functional groups that can be modified and tailored for the specific application. **Figure 12**a shows a schematic of the different methodologies used to produce LNPs with different shapes. These methods include anti-solvent precipitation, interfacial crosslinking, polymerization, sonication, and solvent exchange (Figure 12a).[93] In this section, we summarize the main applications of LNPs in the biomedical field. Figure 12b depicts the interaction of lignin-based nanomaterials with a generic cell (yellow structure at the bottom right of the image).[90] For instance, Alexander et al. doped LNPs with silver ions to prepare a green substitute for antibacterial silver nanoparticles, which provide Ag^+ ions that

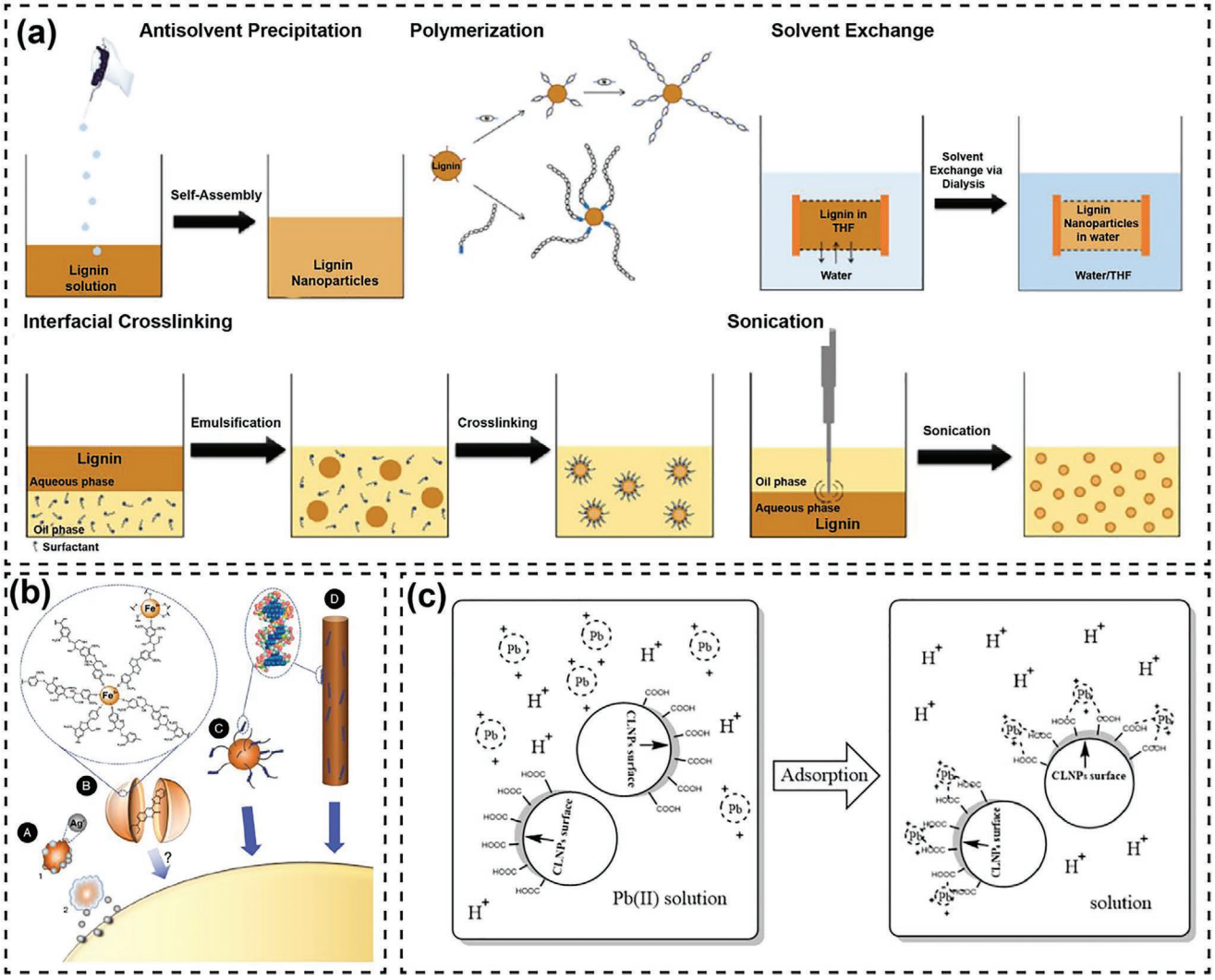

Figure 12. a) Schematic illustration of the various methods used to produce LNPs. Reproduced with permission.[93] Copyright 2018, Elsevier B.V. b) Lignin-based nanomaterials and their interaction with a cell (bottom right of the image). Reproduced with permission.[90] Copyright 2019, Elsevier. c) Schematic illustration of lead absorption on CLNPs. Reproduced under the terms of the CC-BY Creative Commons Attribution 4.0 International license (http://creativecommons.org/licenses/by/4.0/).[114] Copyright 2019, The Authors, published by MDPI.

interfere with basic bacterial cell functions.[110] Another study used the principle of oil-in-water emulsion to synthesize lignin nanocapsules,[111] which rapidly assembled via the π stacking of lignin and its metal chelating ability at alkaline pH. These lignin nanocapsules can be loaded with Coumarin-6. Liu et al. studied lignin-based graft copolymers by atom transfer radical polymerization (ATRP) grafting of 2-(dimethylamino) ethyl methacrylate (DMAEMA).[112] The lignin-PDMAEMA copolymers were studied for DNA binding and gene transfection in cultured cells. These lignin-based copolymers efficiently compacted pDNA into nanoparticles, which is suitable for gene delivery. Solid lignin nanorods and hollow lignin nanotubes were also synthesized using an aluminum film template, which also showed an affinity for DNA.[113]

Adsorption Applications: The inherent properties of lignin have also made it a suitable feedstock for the fabrication of activated carbon and adsorbents. The abundant aromatic structure of lignin means that this feedstock is well suited for developing gas adsorbents.[115] Much research has focused on the production of lignin-derived activated carbon for air pollutant adsorption, such as SO_2, CO_2, and H_2S.[115] Saha et al. developed a nitrogen-doped carbon from lignin that has a CO_2 adsorption capacity at 273 K and 1 bar of 8.6 mmol g^{-1}.[116] In addition, lignin-derived materials have also been used for the adsorption of organic dyes and chemicals such as methylene blue, methyl orange, and phenolics.[117] Fu et al. used steam-activated carbon derived from lignin to remove methylene blue from aqueous solutions.[118] Furthermore, modified lignin materials have been developed for the removal of heavy metals (such as Pb, Cu, Cd, and Zn) and the recovery of noble metals (e.g., Ag, Pd, Au, and Pt).[119] Liu et al. reported the use of carboxyl-modified lignin nanospheres for adsorbing heavy metal ions. The modified lignin nanospheres showed a good Pb(II) adsorption capacity as high as 333.26 mg g^{-1} (Figure 12c).[114] Comprehensive research on lignin-derived materials for adsorption materials has been described in detail recently,[120] and therefore will not be discussed here.

3. Bark-Derived Advanced Materials and Devices

Apart from wood xylem, the bark (outer layer of a tree trunk) is the second most important part of the trunk. Bark in living trees has several distinct physiological and mechanical functions, such as defense against pests, maintaining moisture levels, controlling the trunk girth during seasonal changes, and the protection against fire.[121] Bark is usually considered as a waste material in the timber industry so that it is abundant, renewable, inexpensive, and widely available. In addition to the cellulose, hemicellulose, and lignin existed in wood, bark has other chemical components such as tannin, suberin, rosin, and extractants.[122] This section summarizes recent progress in the field, where representative examples of bark-derived products and applications are discussed, mostly those with multiple functions. To date, the bark of most tree species is mainly used in horticulture and energy production. However, value-added use of bark is attracted increasing attention by the researchers. There are some species of bark that have been widely used in society, such as cork, which is the bark from the cork oak tree. Corks in their natural form are mainly used to manufacture wine stoppers and car interiors in the automotive industry (**Figure 13**a). Some species of bark are also used to produce binderless bark particleboard.[123] In addition, bark-based polyols and bio-oil have been synthesized through liquefaction and pyrolysis, respectively (Figure 13b).[124]

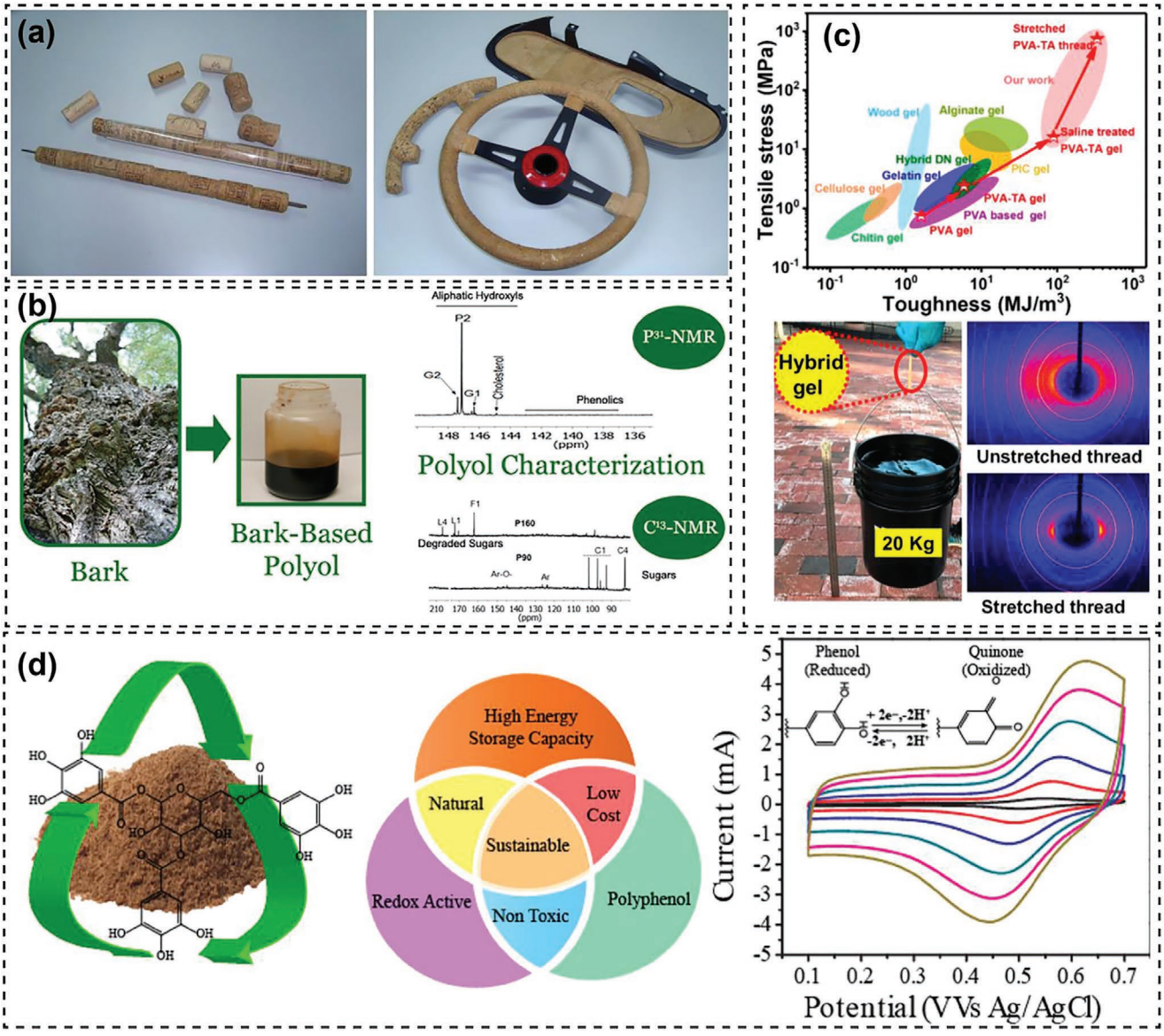

Figure 13. a) Images of cork stoppers, steering wheel, and door panel as representative examples of bark applications. Reproduced under the terms of the CC-BY Creative Commons Attribution 4.0 International license (http://creativecommons.org/licenses/by/4.0/).[123] Copyright 2015, The Authors, published by MDPI. b) Schematic of the process and characterization of bark-based oil. Reproduced with permission.[124] Copyright 2013, American Chemical Society. c) Mechanical performance of PVA-TA hydrogel and the corresponding wide-angle X-ray 2D diffraction images. Reproduced with permission.[125] Copyright 2019, American Chemical Society. d) Schematic of tannin molecules, their advantages for specific applications, and their electrochemical performance. Reproduced with permission.[126] Copyright 2017, American Chemical Society.

Beyond the applications of bulk bark, bark components have been successfully applied in producing bark-based epoxy resins, polyurethane foams, and phenol formaldehyde adhesives.[127,128] Some specific wood species, such as those with high tannin extraction, have many potential applications. Bark tannins have various biological activities, such as antifungal and antioxidant activity,[129] as well as anticancer, antidiabetic, and antifeedant properties.[122] In addition, tannic acid (TA) has been used as a gelation binder to crosslink poly(vinyl alcohol) (PVA) into hydrogels through stepwise physical crosslinking and molecular orientation methods.[125] The obtained hydrogel with aligned PVA fibers showed high mechanical strength of ≈750 MPa (Figure 13c). Furthermore, tannin is considered as the most abundant and versatile redox-active biopolymer in nature.[126] By taking advantage of its high phenol content that can be converted to quinones, tannins are promising energy storage materials. For example, tannins were used as a cathodes for supercapacitors.[126] The CV curves of this device showed prominent redox reaction peaks, which corresponded to the reversible oxidation and reduction of phenolic hydroxyl groups (Figure 13d). The introduction of tannin as a redox active substance provides an excellent opportunity to develop sustainable energy storage systems.

4. Leaf-Derived Advanced Materials and Devices

The tree leaf is capable to harvest solar energy and transport this energy to reaction centers in the tree for catalytic conversion of chemical species, while itself remains flexible and lightweight.[130] Similar use of solar energy by chemical synthesis is a long-standing aim for the chemical community. The transpiration of plants, especially the evaporation of water from leaves, accounts for a large portion of the total precipitation on the continent and affects the global water distribution and climate.[131] They contain various components, such as polyphenols, plant pigments, and proteins that can provide active sites for adsorption; as well as other extractives that have antimicrobial, antipyretic and osteogenic activity, and other medicinal value.[132] These inherent features provide great potential for the application of leaves. In this review, we will not discuss the medicinal value of leaves and leaf extracts; we focus on leaf-based materials and products in the fields of environment, catalysis, and energy.

4.1. Adsorption

Biosorption is a method that uses inexpensive biomass to chelate toxic heavy metals and remove dyes, in particularly, it is suitable for removing pollutants from industrial wastewater. In addition to the lignin discussed in Section 2.3.3, which is widely used for environmental adsorption, various kinds of biomass can also be used for biosorption processes, such as leaves, microorganisms, and sawdust. Tree leaves (**Figure 14**a) are an attractive biomass as they are inexpensive, effective, and abundantly available.[133] They contain a variety of ingredients, such as plant pigments, polyphenols, and proteins, which provide active sites for binding heavy metals. In previous research, various leaves were used to adsorb heavy metals, including Cr, Ni, Cu, Pb, and Cd.[134,135] Arunima et al. used Neem leaf powder as a biosorbent to remove Cd(II) from aqueous solutions.[134] Figure 14b shows the irregular morphology of fine particles of leaf powder adsorbent, which showed good adsorption behavior in alkaline media. Another study showed that leaf powder had good biosorption performance for removing Cu(II) from aqueous solutions, with a removal fraction up to 85.92% (Figure 14c).[135]

4.2. Energy

As the demand for supercapacitors and lithium batteries continues to grow, researchers have invested significant efforts in developing advanced electrode materials with high specific capacity/capacitance and long cycle life. Similar to other biomass materials, leaves are a naturally abundant carbon source. Among the various carbon materials, porous carbon has been widely used as an electrode material. In recent years, the production of porous carbon from leaves has been attracting increasing interest. Chuang et al. were inspired by the unique functions and tissue structure of leaves, and proposed natural carbonized leaves (CL) as polysulfide diffusion inhibitors in lithium–sulfur (Li–S) batteries (Figure 14d).[136] The free-standing CL films had an anatomically hierarchical layered microstructure, which is critical for intercepting polysulfides migration. Additionally, the CL had an integral carbon skeleton, rich micro/mesoporous space, and an internal macroporous network for storing captured active materials, transporting electrons, and absorbing electrolytes. The unique microstructure of CL resulted in a high coulombic efficiency above 98% and good cyclability over 150 cycles. In another study, nitrogen-doped porous carbon nanosheets were prepared from tree leaves by carbonization and activation.[137] The porous carbon was used as an electrode material for lithium batteries and supercapacitors, which both showed outstanding electrochemical performance.

Interestingly, Jie et al. developed a leaf-based triboelectric nanogenerator (Leaf-TENG), which uses green leaves as charged layers and electrodes to efficiently collect mechanical energy.[138] Leaf-TENG showed a maximum output power of ≈45 mW m^{-2}, which was sufficient to drive LEDs (Figure 14e). In addition, interests in leaf-derived materials as solar absorbers have greatly increased in recent years. Zhuang et al. showed for the first time that the design of solar-absorber-leaf interfaces can also increase or suppress transpiration efficiency, extending the concept of solar vapor generation at the interface to adjustable plant transpiration (Figure 14f).[139]

4.3. Catalysis

Metal nanoparticles have found widespread applications as antibacterial and therapeutic agents, microelectronics, catalysis, and topical ointments and creams.[140] Various methods were studied for metal nanoparticle syntheses, such as electrochemical and photochemical reduction, chemical methods, heat evaporation, and microwave-assisted processes.[141] However, these methods are not cost-effective, require hazardous chemicals and high energy input, and have

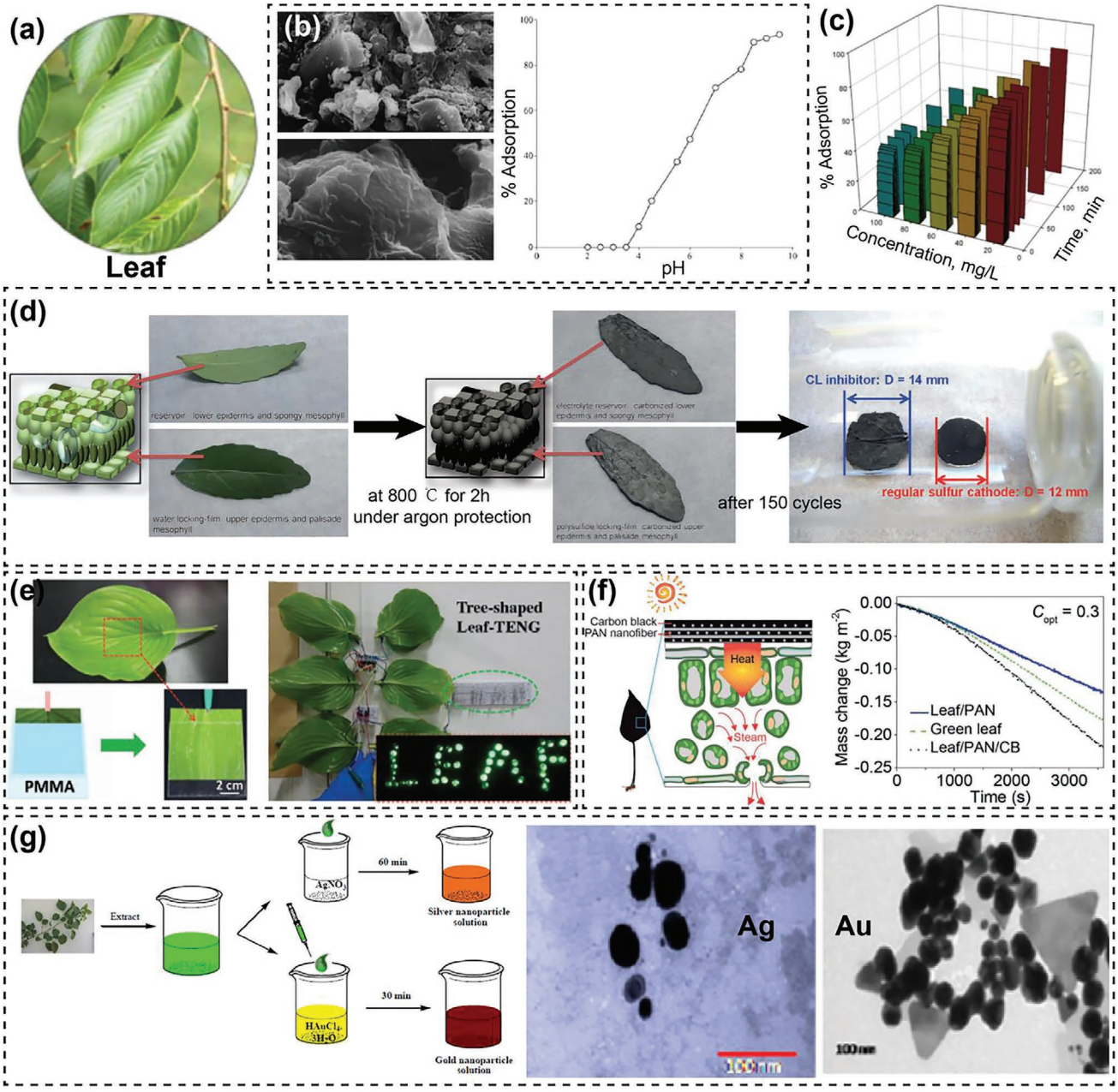

Figure 14. a) Image of a green leaf. Reproduced with permission.[133] Copyright 2016, Elsevier B.V. b) SEM images of leaf powder, along with their adsorption capacity as a function of pH. Reproduced with permission.[134] Copyright 2005, Elsevier B.V. c) Cu adsorption performance of leaf powder as a function of concentration and time. Reproduced with permission.[135] Copyright 2006, Elsevier B.V. d) Schematic illustration of the fabrication process for CLs. Reproduced with permission.[136] Copyright 2014, Wiley-VCH. e) Schematic of the fabrication process of leaf-TENG assembled using green leaves and poly(methyl methacrylate) (PMMA), showing that leaf-TENG can drive LEDs. Reproduced with permission.[138] Copyright 2018, Wiley-VCH. f) Schematic of the fabrication process of leaf absorbers and their evaporation performance over time. Reproduced under the terms of the CC-BY Creative Commons Attribution 4.0 International license (https://creativecommons.org/licenses/by/4.0).[139] Copyright 2017, The Authors, published by Wiley-VCH. g) Schematic of the fabrication process of silver and gold nanoparticles using leaf extracts, along with the corresponding SEM images of the produced Ag and Au nanoparticles. Reproduced with permission.[143] Copyright 2012, VBRI Press.

low material conversion. Ecofriendly approaches using plant leaf extract for metal nanoparticle synthesis have been developed as effective alternatives to chemical approaches. These new approaches use aqueous extracts with high reduction capacities that are obtained from leaves.[140,142] Several tree-leaf extracts have been successfully used for synthesis of metal nanoparticles, such as *Dalbergia sissoo* extract, which was used to prepare spherical gold (50–80 nm) and silver nanoparticles (5–55 nm) at ambient temperature (Figure 14g).[143] In addition, Amla leaf extract has been used to synthesize silver (10–20 nm) and gold (15–25 nm) nanoparticles.[144] Awward et al. prepared copper hydroxide nanowires using sodium

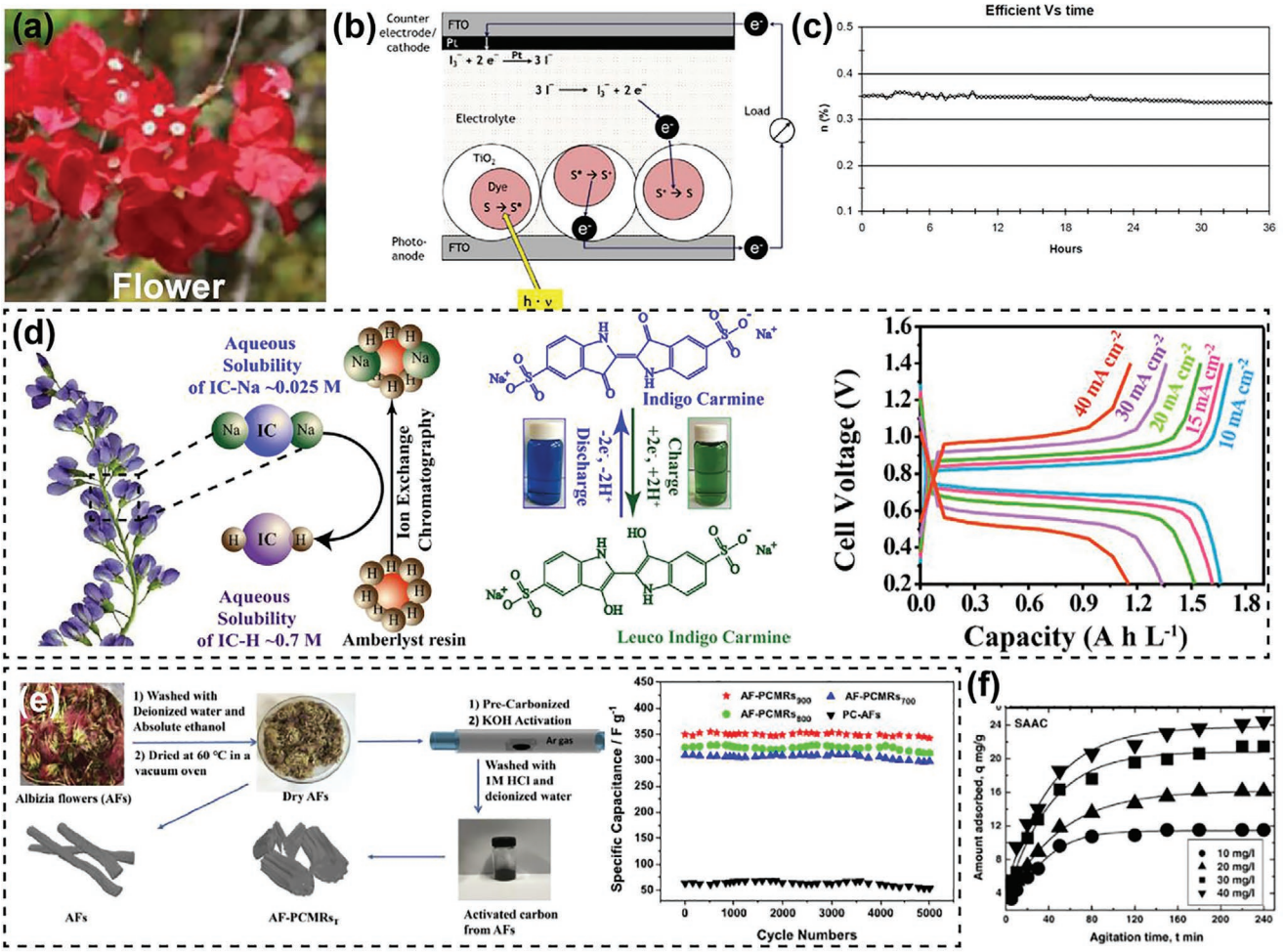

Figure 15. a) Representative image of red flowers from a tree. Reproduced with permission.[145] Copyright 2015, Elsevier B.V. b) Schematic of the operational process of a dye-sensitized solar cells (DSSC). Reproduced with permission.[148] Copyright 2014, Elsevier Ltd. c) Time dependence of the efficiency of a DSCC using flower-extract dye. Reproduced under the terms of the CC-BY Creative Commons Attribution 3.0 Unported license (https://creativecommons.org/licenses/by/3.0/).[149] Copyright 2011, The Authors, published by MDPI. d) Schematic of the dye extracted from the indigo fera plant, along with the ion exchange mechanism of IC-Na and IC-H, and its performance when used in a flow battery. Reproduced with permission.[150] Copyright 2019, American Chemical Society. e) Schematic of the process for preparing supercapacitor electrode materials and their cycle stability. Reproduced with permission.[151] Copyright 2019, Elsevier B.V. f) Adsorption properties of crystal violet. Reproduced with permission.[152] Copyright 2006, Elsevier B.V.

hydroxide and copper chloride dehydrates from pistachio leaf extract at ambient temperature.[142]

5. Flower-Derived Advanced Materials and Devices

Generally, tree flowers are used for horticultures (**Figure 15**a),[145] although they have a wide variety of applications. Several dyes can be extracted from flower pigments, including anthocyanins, flavonoid, and carotenoids, which can be used as red, yellow, violet, and blue colors.[146] In addition, flowers are natural sources of antioxidants because they are rich in phenolic components, which have anticarcinogenic, antimutagenic, anti-inflammation, and antioxidant activities.[147] It is well known that degenerative and pathological processes, including atherosclerosis, aging, and cancer in humans, are caused by oxidative damage. Some tree flowers are used in traditional functional food and medicine due to their antioxidant activity, while others have little medicinal value. In general, there are two main ways to achieve value-added utilization of the tree flowers: 1) dye extracted from flowers is used as light-harvesting materials and redox materials in the field of energy storage; 2) one-step pyrolysis and activation treatment of flowers to obtain activated carbon that can be used in the fields of environment adsorption and energy storage.

5.1. Dye Applications in Energy Harvesting and Storage

Natural dyes, exacted from tree flowers, can be used as the sensitizer in dye sensitized solar cells (DSSC). Natural dyes have a donor-π-conjugated bridge-acceptor structure, which enables fast and energetically optimized charge transfer. As shown in Figure 15b, dyes harvest incident photons from light and get

excited from the ground state (S) to the excited state (S*) and release electrons, which are injected into the conduction band of TiO_2 and result in the oxidation of dyes (S^+). Then, S^+ accept electrons from the redox mediator (I—ions) and return to S. Dye sensitizers are classified as inorganic dyes, organic dyes, and metal–organic dyes. Among them, ruthenium bipyridyl compounds are the most successful due to their high conversion efficiency ($\eta > 10\%$) and stability, but require the expensive raw material (Ru), and involve multistep and time-consuming preparation procedures. Natural dyes used in DSSC normally have $\eta < 1\%$, which is relatively low as compared to synthetic dyes.[148] Hernandez-Martinez et al. used Bougainvillea extract as a sensitizer in DSSC with a η of 0.48% and a current density of 2.29 mA cm^{-2} (Figure 15c), where the low η was because of poor interaction between TiO_2 and the dye.[149] However, nature dyes are a promising alternative to synthetic dyes due to their large absorption coefficients in the visible region, accessibility, easy preparation, low cost, and environmentally friendliness.

Natural dyes have also been used as environmentally friendly and sustainable reactive substances in battery electrolytes because of their redox properties. Mukhopadhyay et al. used natural dye (5,5′-indigodisulfonic acid sodium salt) (IC-Na) extracted from the flower of the indigofera plant, as a redox active anolyte in an aqueous organic redox flow battery (Figure 15d).[150] To improve the poor solubility of IC-Na, 5,5′-indigodisulfonic acid (IC-H) was obtained through ion exchange resulting in a 22-fold increase of the solubility in 0.1 M $HClO_4$ solution. The improved IC-H dye had a voltage window of 0.85 V, an energy density of 20.6 W h L^{-1}, and a power density of 48 mW cm^{-2} at 40 mA cm^{-2} current density, when paired with bromine/hydrobromic acid (Br_2/HBr) catholyte.

5.2. Carbonized Flower-Derived Materials

Compared with other carbonized biomass or tree parts, carbonized flowers have unique morphologies and pore structures. Wu et al. used carbonized flowers to prepare hierarchical porous carbon microrods for high-performance supercapacitors via one-step pyrolysis and activation treatment (Figure 15e).[151] They obtained carbon microrods with high specific area (2757.63 m^2 g^{-1}) and pore volume (1.47 cm^3 g^{-1}), which gave a high specific capacitance of 406 F g^{-1} at 0.5 A g^{-1} in 6 M KOH electrolyte and a good rate capability of 86.1%. In another study, active carbon prepared from male flowers of coconut trees with a porosity of 65% and surface area of 55.6 m^2 g^{-1} showed high adsorption capacity of 85.84 mg g^{-1} for crystal violet (Figure 15f).[152]

6. Seed-Derived Advanced Materials and Devices

The main use of the seeds in the fruit is still plant reproduction, while seeds are increasingly used in our daily lives. Seeds are a cheap and renewable raw material, which could be collected from the trees in autumn as it matures, even over the winter to early spring. Seeds that contain viscous oil, such as *Jatropha* seeds, tallow tree seeds, and olive seeds, are used for making soap and candles. In the cosmetics industry, the viscous oil from seeds are used as a diesel/paraffin substitute or extender, for treating skin diseases, and to soothe pain caused by rheumatism.[153,154] Various methods have been used for extracting oils from these oilseeds, including mechanical pressing, supercritical fluids, organic solvents, ultrasound, and microwave-assisted extraction.[154] In the following section, we summarize current and potential applications of various types of seeds, and seed waste after oil extraction, such as components extracted from seeds to fabricate advanced materials and devices, carbon-based materials from seeds or seed waste for energy and environmental applications.

6.1. Seed Extracts for Advanced Materials and Devices

The rapid technological development has greatly reduced life expectancy of consumer electronics, meanwhile, an increasing number of electronic waste has been produced due to the nondegradable materials for device fabrication. Recently, the utilization of natural renewable biomaterials as the substrate for electronics fabrication has attracted extensive attention. However, lots of degradable biomaterials are not shape-stable in organic solvents, which is a big challenge for the electronics fabrication and limits their practical applications. To address this issue, polysaccharides from renewable bio-based materials have attracted more attention in recent years. There are different sources of polysaccharides, including seaweed extracts, tree cell wall materials (cellulose and hemicellulose), and tree seeds. Polysaccharide extracts from tree seeds have also been used to develop advanced materials and electronic devices. Yi et al. developed water-soluble and high-performance transient sensors on a galactomannan (GM) substrate.[155] In this study, the GM was extracted from the endosperm of dicotyledonous seeds, such as L. *leucocephala*, *Sesbania cannabina*, and *Cyamopsis tetragonoloba* (**Figure 16**a). They used simple and cost-effective extraction and purification methods to fabricate GM films as biodegradable substrates. The zinc-based sensors on the degradable galactomannan substrate endowed with high-performance, including high-precision temperature measurement and high-fidelity electrophysiological signal monitoring (Figure 16b). The baseline drift of electrocardiogram (ECG) signals collected from copper and zinc electrodes was due to breathing or body movement (Figure 16c). More importantly, the resulting sensors were stable in organic solutions while they were fully soluble in water, which make it highly promising to be extensively applied in green electronics fields. Tamarind seed polysaccharide (TSP)-based proton conducting biopolymer membranes have also been reported.[156] Figure 16d shows a transparent thin film of pure TSP biopolymer. The electrical conductivity was controlled by NH_4SCN doping of the TSP films. The primary proton battery had an open circuit voltage of 1.51 V for the highest conductivity film. This TSP film has great potential in the application of electrochemical devices.

6.2. Carbon-Based Materials

Tree seeds are another carbon source derived from biomass that can be used to produce carbon-based materials. In this section,

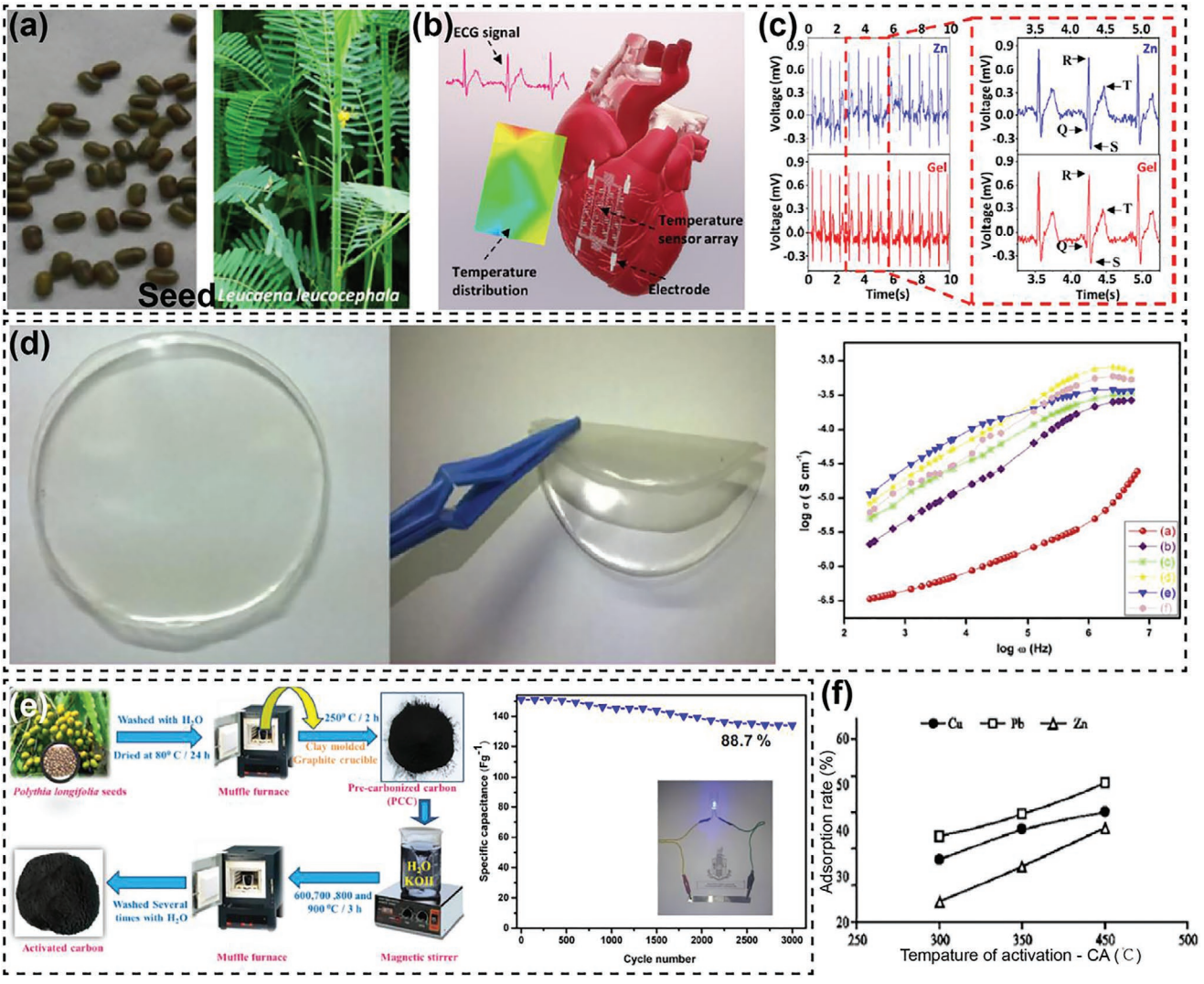

Figure 16. a) Photographs of the seeds and leaves of *L. leucocephala*. b) Sensors can be placed on the heart to potentially diagnose arrhythmia and c) ECG signals collected from the electrode of the heart sensor. a–c) Reproduced with permission.[155] Copyright 2018, American Chemical Society. d) Photographs of the transparent seed-polysaccharide film and its corresponding conductance spectra. Reproduced with permission.[156] Copyright 2016, Elsevier B.V. e) Schematic of the fabrication process for seed-based activated carbon and cyclic stability of the supercapacitor (inset: PLS-AC device setup). Reproduced with permission.[157] Copyright 2019, Elsevier B.V. f) The ability of seed-based activated carbon to adsorb heavy metal ions with temperature changes. Reproduced with permission.[158] Copyright 2006, Asian Network for Scientific Information.

we summarize carbon-based materials from seeds and seed waste for energy and environmental applications. Recently, Srinivasan et al. reported a polyalthia longifolia seed (PLS)-derived activated carbon (AC) that was synthesized by pyrolytic chemical activation (Figure 16e).[157] The prepared PLS-AC samples were studied for their performance as electrode materials in supercapacitors, which showed stable cycling up to 3000 cycles at 2 A g^{-1} and good capacitance retention of 88.7% (Figure 16e). In addition, seed-derived AC has also been used in environmental pollution adsorption. For example, AC prepared from seed shells of palm trees was used for removing heavy metals from aqueous solutions.[158] Increasing the activation temperature opened new pores accessible to metal ions, which facilitates adsorption of heavy metals (Figure 16f). Another study has investigated the adsorption of phenols from wastewater using date seed carbon (DSC).[159] These results displayed that seed-derived AC has a wide range of industrial applications, such as energy storage and adsorption of metal ions and organic pollutants.

7. Root-Derived Advanced Materials and Devices

Our perception of plants is mainly based on their visible parts, such as the trunk, branches, and leaves, while the underground root system is often hidden. Globally, forests account for 4 billion hectares that is 30% of the Earth's land surface, where 20–40% of forest biomass consists of roots.[160] Roots play a key role in tree growth, as they absorb water and nutrients from the soil, store carbon compounds, and provide physical stability. The root system is a complex 3D network that varies among plant species

Table 1. Different tree-based materials and their novel applications.

Tree section	Components and structures	Applications	Reference
Wood	Chips and blocks	Energy storage, environment, solar evaporation, multifunctional materials, etc.	[5–7,16,18]
	Cellulose	Energy storage, membrane, electronics, environment, biomedical, composites, etc.	[10,32,37,44,58]
	Hemicellulose	Biomedical, packaging, membrane, paper coating, etc.	[60,80,82,83]
	Lignin	Energy storage, environment, biomedical, binder, composites, etc.	[1,91,93,95,97]
Bark	Aromatic polymer	Bio-oil, epoxy resins, polyurethane foams	[124,127]
	Tannin	Super strong and tough hydrogel	[125]
		Supercapacitors	[126,163]
		Biosorbents	[164]
Leaf	Pigments polyphenols	Biosorption	[135]
	Carbon derived from leaves through carbonization	Li-ion batteries	[136,165]
		Supercapacitors	[137,166]
	Structural design based on leaves	Leaf-TENG	[138]
		Solar vapor generation	[139]
	Leaf extract	Catalysis	[143,167]
		Biomedical	[133]
Flower	Dye	Flow batteries	[150]
		Li-ion batteries	[168]
		Solar cell	[148,149]
	Carbon derived from flowers through carbonization	Supercapacitors	[151,169]
		Zinc–air batteries	[170]
		Adsorption	[152]
	Flower extract	Biomedical	[147]
Seed	Polysaccharides	Electronics	[155]
		Biomedical	[171]
	Carbon derived from seeds through carbonization	Supercapacitors	[157]
		Adsorption	[159]
Root	Root extract	Biomedical	[172]

by age, root system type, branching pattern, orientation, interface properties with the soil, and diameter.[161] Despite advances in root system research in recent decades, most of these studies focus on physical and chemical properties of root and root–soil interactions.[162] Other applications include handicrafts carved from tree roots, medicinal from many roots (e.g., banyan, neem, moringa). However, little research has been done on the functional materials based on tree roots. It is certaintly that great values can be added to the forest industry if functional materials could be prepared from tree roots in the future.

8. Conclusions and Perspectives

Herein, the recent achievements in bioderived materials from different parts of trees for sustainable functional materials have been systematically reviewed. As summarized in **Table 1**, the applications of the different parts of trees vary with their chemical components and structures. Traditionally, wood-based products have been used in construction, furniture, transportation, combustion, and paper manufacturing. Recently, the inherent structures and components of wood have been further explored for material functionalization and device fabrication, including hierarchical architectures and mesoporous structures, anisotropic cell wall alignments, chemical features of molecules, and hydrogen bondings, etc. Biopolymers from trees have their unique characteristics. For instance, nanocellulose has been applied as building blocks to design various advanced materials and configurations with widespread applications in the energy, electronics, and biomedical fields. Hydrophobization can promote many industrial applications of hemicellulose. Recent works have shown that hemicellulose after hydrophobization can be widely used in biomedical field (e.g., wound dressings and drug release systems) and transportation packaging field. Moreover, the use of lignin through synthetic polymers is preferable in the production of nanomaterials for drug delivery and other biomedical fields. Tannin in bark, and dye extracted from flowers have also

been used in energy storage due to their aromatic structures and various active groups that provide reversible redox sites. Polysaccharides from seeds have excellent film formability and biocompatibility, which has attracted much interest in biomedical research. Leaf extracts with good reducibility have been developed for metal nanoparticle synthesis. Furthermore, components in the different parts of the tree can be used to make activated carbon by carbonization, which has potential applications in energy storage and environmental adsorption fields.

Even though the relationship of materials, structure, performance, and applications of biopolymers from trees is studied in various research fields, due to the significant variations of cell geometries in different tree types and even the same tree type from different areas, the structures and components could be very different. Wood diversity with suitable microstructures, therefore, should be further considered in wood-based matters and devices. There are various efforts that need to be made to commercialize the structures and materials from trees for new applications, including: 1) developing environmentally friendly and green pathways for producing tree-based derivatives or sustainable functional materials; 2) increasing the scalability, lifetime and durability of materials and devices to ensure that they provide sufficiently high performance for the intended applications; 3) developing technologies for the full utilization of components and structures derived from nontimber products, such as bark, leaf, flower, seed, and root; and 4) developing well-established standards for characterizations. We expect that future studies will provide more exciting ideas and inspirations of tree-based materials with outstanding performance for immense applications.

Acknowledgements

The authors acknowledge the funding resources of the program of Electronics, Photonics and Magnetic Devices in the Division of Electrical, Communications and Cyber Systems in the National Science Foundation (Award Number: 1933072) and the Northeastern University Tier 1 grant fund to H.Z.

Conflict of Interest

The authors declare no conflict of interest.

Keywords

bioderived materials, bioinspired design, functionality, sustainability, trees

Received: March 8, 2020
Revised: May 15, 2020
Published online:

[1] H. Wang, Y. Pu, A. Ragauskas, B. Yang, *Bioresour. Technol.* **2019**, *271*, 449.

[2] a) L. R. Lynd, J. H. Cushman, R. J. Nichols, C. E. Wyman, *Science* **1991**, *251*, 1318; b) L. R. Lynd, M. S. Laser, D. Bransby, B. E. Dale, B. Davison, R. Hamilton, M. Himmel, M. Keller, J. D. McMillan, J. Sheehan, *Nat. Biotechnol.* **2008**, *26*, 169.

[3] S. P. Chundawat, B. S. Donohoe, L. da Costa Sousa, T. Elder, U. P. Agarwal, F. Lu, J. Ralph, M. E. Himmel, V. Balan, B. E. Dale, *Energy Environ. Sci.* **2011**, *4*, 973.

[4] E. Kintisch, *Science* **2007**, *316*, 1827.

[5] J. Huang, B. Zhao, T. Liu, J. Mou, Z. Jiang, J. Liu, H. Li, M. Liu, *Adv. Funct. Mater.* **2019**, *29*, 1902255.

[6] H. Zhu, Z. Fang, C. Preston, Y. Li, L. Hu, *Energy Environ. Sci.* **2014**, *7*, 269.

[7] S. He, C. Chen, Y. Kuang, R. Mi, Y. Liu, Y. Pei, W. Kong, W. Gan, H. Xie, E. Hitz, *Energy Environ. Sci.* **2019**, *12*, 1558.

[8] a) T. Li, Y. Zhai, S. He, W. Gan, Z. Wei, M. Heidarinejad, D. Dalgo, R. Mi, X. Zhao, J. Song, *Science* **2019**, *364*, 760; b) Y. Kuang, C. Chen, S. He, E. M. Hitz, Y. Wang, W. Gan, R. Mi, L. Hu, *Adv. Mater.* **2019**, *31*, 1900498.

[9] a) X. Zhao, H. Chen, F. Kong, Y. Zhang, S. Wang, S. Liu, L. A. Lucia, P. Fatehi, H. Pang, *Chem. Eng. J.* **2019**; b) D. Klemm, F. Kramer, S. Moritz, T. Lindström, M. Ankerfors, D. Gray, A. Dorris, *Angew. Chem., Int. Ed.* **2011**, *50*, 5438; c) N. Lin, J. Huang, A. Dufresne, *Nanoscale* **2012**, *4*, 3274.

[10] H. Zhu, W. Luo, P. N. Ciesielski, Z. Fang, J. Zhu, G. Henriksson, M. E. Himmel, L. Hu, *Chem. Rev.* **2016**, *116*, 9305.

[11] R. J. Moon, A. Martini, J. Nairn, J. Simonsen, J. Youngblood, *Chem. Soc. Rev.* **2011**, *40*, 3941.

[12] F. F. Kollmann, E. W. Kuenzi, A. J. Stamm, *Principles of Wood Science and Technology: II Wood Based Materials*, Springer Science & Business Media, Berlin, Germany **2012**.

[13] a) T. Li, S. X. Li, W. Kong, C. Chen, E. Hitz, C. Jia, J. Dai, X. Zhang, R. Briber, Z. Siwy, *Sci. Adv.* **2019**, *5*, eaau4238; b) F. Shen, W. Luo, J. Dai, Y. Yao, M. Zhu, E. Hitz, Y. Tang, Y. Chen, V. L. Sprenkle, X. Li, *Adv. Energy Mater.* **2016**, *6*, 1600377.

[14] T. Li, X. Zhang, S. D. Lacey, R. Mi, X. Zhao, F. Jiang, J. Song, Z. Liu, G. Chen, J. Dai, *Nat. Mater.* **2019**, *18*, 608.

[15] a) W. Luo, Y. Zhang, S. Xu, J. Dai, E. Hitz, Y. Li, C. Yang, C. Chen, B. Liu, L. Hu, *Nano Lett.* **2017**, *17*, 3792; b) J. Luo, X. Yao, L. Yang, Y. Han, L. Chen, X. Geng, V. Vattipalli, Q. Dong, W. Fan, D. Wang, *Nano Res.* **2017**, *10*, 4318; c) J.-H. Kim, J.-H. Kim, E.-S. Choi, H. K. Yu, J. H. Kim, Q. Wu, S.-J. Chun, S.-Y. Lee, S.-Y. Lee, *J. Power Sources* **2013**, *242*, 533.

[16] J. Song, C. Chen, S. Zhu, M. Zhu, J. Dai, U. Ray, Y. Li, Y. Kuang, Y. Li, N. Quispe, *Nature* **2018**, *554*, 224.

[17] D. Brack, Background study prepared for the thirteenth session of the United Nations Forum on Forests; available from https://www.un.org/esa/forests/wp-content/uploads/2018/04/UNFF13_BkgdStudy_ForestsSCP.pdf.

[18] F. Jiang, T. Li, Y. Li, Y. Zhang, A. Gong, J. Dai, E. Hitz, W. Luo, L. Hu, *Adv. Mater.* **2018**, *30*, 1703453.

[19] a) C.-H. Zhou, X. Xia, C.-X. Lin, D.-S. Tong, J. Beltramini, *Chem. Soc. Rev.* **2011**, *40*, 5588; b) J. Zakzeski, P. C. Bruijnincx, A. L. Jongerius, B. M. Weckhuysen, *Chem. Rev.* **2010**, *110*, 3552.

[20] S. Y. Oh, D. I. Yoo, Y. Shin, H. C. Kim, H. Y. Kim, Y. S. Chung, W. H. Park, J. H. Youk, *Carbohydr. Res.* **2005**, *340*, 2376.

[21] S. Hokkanen, A. Bhatnagar, M. Sillanpää, *Water Res.* **2016**, *91*, 156.

[22] J. Zhu, X. Zhuang, *Prog. Energy Combust. Sci.* **2012**, *38*, 583.

[23] M. Jorfi, E. J. Foster, *J. Appl. Polym. Sci.* **2015**, 132.

[24] a) J. R. Capadona, O. Van Den Berg, L. A. Capadona, M. Schroeter, S. J. Rowan, D. J. Tyler, C. Weder, *Nat. Nanotechnol.* **2007**, *2*, 765; b) Y. Nishiyama, J. Sugiyama, H. Chanzy, P. Langan, *J. Am. Chem. Soc.* **2003**, *125*, 14300.

[25] J.-H. Kim, B. S. Shim, H. S. Kim, Y.-J. Lee, S.-K. Min, D. Jang, Z. Abas, J. Kim, *Int. J. Precision Eng. Manuf.-Green Technol.* **2015**, *2*, 197.

[26] F. Kolpak, J. Blackwell, *Macromolecules* **1976**, *9*, 273.

[27] a) B. Lee, *Opt. Fiber Technol.* **2003**, *9*, 57; b) V. Bhatia, A. M. Vengsarkar, *Opt. Lett.* **1996**, *21*, 692; c) L. Hu, M. Pasta, F. La

Mantia, L. Cui, S. Jeong, H. D. Deshazer, J. W. Choi, S. M. Han, Y. Cui, *Nano Lett.* **2010**, *10*, 708; d) X. Xie, M. Ye, L. Hu, N. Liu, J. R. McDonough, W. Chen, H. N. Alshareef, C. S. Criddle, Y. Cui, *Energy Environ. Sci.* **2012**, *5*, 5265.
[28] a) S. Eichhorn, G. Davies, *Cellulose* **2006**, *13*, 291; b) K. Tashiro, M. Kobayashi, *Polymer* **1991**, *32*, 1516.
[29] P. Mohammadi, M. S. Toivonen, O. Ikkala, W. Wagermaier, M. B. Linder, *Sci. Rep.* **2017**, *7*, 1.
[30] S. Hooshmand, Y. Aitomäki, N. Norberg, A. P. Mathew, K. Oksman, *ACS Appl. Mater. Interfaces* **2015**, *7*, 13022.
[31] L. Deng, R. J. Young, I. A. Kinloch, Y. Zhu, S. J. Eichhorn, *Carbon* **2013**, *58*, 66.
[32] O. Nechyporchuk, R. Bordes, T. Köhnke, *ACS Appl. Mater. Interfaces* **2017**, *9*, 39069.
[33] C. M. Clarkson, S. M. El Awad Azrak, R. Chowdhury, S. N. Shuvo, J. Snyder, G. Schueneman, V. Ortalan, J. P. Youngblood, *ACS Appl. Polym. Mater.* **2019**, *1*, 160.
[34] A. Walther, J. V. Timonen, I. Díez, A. Laukkanen, O. Ikkala, *Adv. Mater.* **2011**, *23*, 2924.
[35] a) K. Bachmann, *Book Paper Ann.* **1983**, *2*, 3; b) H. Yousefi, T. Nishino, M. Faezipour, G. Ebrahimi, A. Shakeri, *Biomacromolecules* **2011**, *12*, 4080; c) M. Nogi, H. Yano, *Appl. Phys. Lett.* **2009**, *94*, 233117; d) H. Yano, S. Sasaki, M. I. Shams, K. Abe, T. Date, *Adv. Opt. Mater.* **2014**, *2*, 231.
[36] H. Fukuzumi, T. Saito, T. Iwata, Y. Kumamoto, A. Isogai, *Biomacromolecules* **2009**, *10*, 162.
[37] M. Nogi, S. Iwamoto, A. N. Nakagaito, H. Yano, *Adv. Mater.* **2009**, *21*, 1595.
[38] H. Zhu, Z. Fang, Z. Wang, J. Dai, Y. Yao, F. Shen, C. Preston, W. Wu, P. Peng, N. Jang, *ACS Nano* **2016**, *10*, 1369.
[39] J. Chen, M. Akin, L. Yang, L. Jiao, F. Cheng, P. Lu, L. Chen, D. Liu, H. Zhu, *ACS Appl. Mater. Interfaces* **2016**, *8*, 27081.
[40] B. Zhou, Z. Zhang, Y. Li, G. Han, Y. Feng, B. Wang, D. Zhang, J. Ma, C. Liu, *ACS Appl. Mater. Interfaces* **2020**, *12*, 4895.
[41] Y. Wang, H. Lai, Z. Cheng, H. Zhang, E. Zhang, T. Lv, Y. Liu, L. Jiang, *Nanoscale* **2019**, *11*, 8984.
[42] M. Matsumoto, T. Kitaoka, *Adv. Mater.* **2016**, *28*, 1765.
[43] X.-F. Zhang, Y. Feng, Z. Wang, M. Jia, J. Yao, *J. Membr. Sci.* **2018**, *568*, 10.
[44] A. Mukhopadhyay, Z. Cheng, A. Natan, Y. Ma, Y. Yang, D. Cao, W. Wang, H. Zhu, *Nano Lett.* **2019**, *19*, 8979.
[45] Z. Cheng, H. Ye, F. Cheng, H. Li, Y. Ma, Q. Zhang, A. Natan, A. Mukhopadhyay, Y. Jiao, Y. Li, *Adv. Mater. Interfaces* **2019**, *6*, 1802010.
[46] Z. Cheng, Y. Ma, L. Yang, F. Cheng, Z. Huang, A. Natan, H. Li, Y. Chen, D. Cao, Z. Huang, *Adv. Opt. Mater.* **2019**, *7*, 1801816.
[47] O. Kose, A. Tran, L. Lewis, W. Y. Hamad, M. J. MacLachlan, *Nat. Commun.* **2019**, *10*, 510.
[48] M. Pääkkö, J. Vapaavuori, R. Silvennoinen, H. Kosonen, M. Ankerfors, T. Lindström, L. A. Berglund, O. Ikkala, *Soft Matter* **2008**, *4*, 2492.
[49] N. Lavoine, L. Bergström, *J. Mater. Chem. A* **2017**, *5*, 16105.
[50] a) N. T. Cervin, E. Johansson, P. A. Larsson, L. Wågberg, *ACS Appl. Mater. Interfaces* **2016**, *8*, 11682; b) W. Chen, Q. Li, Y. Wang, X. Yi, J. Zeng, H. Yu, Y. Liu, J. Li, *ChemSusChem* **2014**, *7*, 154.
[51] F. Jiang, Y.-L. Hsieh, *J. Mater. Chem. A* **2014**, *2*, 6337.
[52] H. Sehaqui, Q. Zhou, L. A. Berglund, *Compos. Sci. Technol.* **2011**, *71*, 1593.
[53] a) Y. Kobayashi, T. Saito, A. Isogai, *Angew. Chem., Int. Ed.* **2014**, *53*, 10394; b) B. Seantier, D. Bendahou, A. Bendahou, Y. Grohens, H. Kaddami, *Carbohydr. Polym.* **2016**, *138*, 335.
[54] B. Wicklein, A. Kocjan, G. Salazar-Alvarez, F. Carosio, G. Camino, M. Antonietti, L. Bergström, *Nat. Nanotechnol.* **2015**, *10*, 277.
[55] L. Yang, A. Mukhopadhyay, Y. Jiao, Q. Yong, L. Chen, Y. Xing, J. Hamel, H. Zhu, *Nanoscale* **2017**, *9*, 11452.
[56] D. Cao, Y. Xing, K. Tantratian, X. Wang, Y. Ma, A. Mukhopadhyay, Z. Cheng, Q. Zhang, Y. Jiao, L. Chen, *Adv. Mater.* **2019**, *31*, 1807313.
[57] a) J. Liu, F. Cheng, H. Grénman, S. Spoljaric, J. Seppälä, J. E. Eriksson, S. Willför, C. Xu, *Carbohydr. Polym.* **2016**, *148*, 259; b) T. Lu, Q. Li, W. Chen, H. Yu, *Compos. Sci. Technol.* **2014**, *94*, 132.
[58] Y. Qi, Z. Cheng, Z. Ye, H. Zhu, C. Aparicio, *ACS Appl. Mater. Interfaces* **2019**, *11*, 27598.
[59] J. Rao, H. Gao, Y. Guan, W.-q. Li, Q. Liu, *Carbohydr. Polym.* **2019**, *208*, 513.
[60] W. Farhat, R. A. Venditti, M. Hubbe, M. Taha, F. Becquart, A. Ayoub, *ChemSusChem* **2017**, *10*, 305.
[61] I. Egüés, C. Sanchez, I. Mondragon, J. Labidi, *Bioresour. Technol.* **2012**, *103*, 239.
[62] Q. A. Nguyen, M. P. Tucker, F. A. Keller, F. P. Eddy, *Appl. Biochem. Biotechnol.* **2000**, *84*, 561.
[63] I. Hasegawa, K. Tabata, O. Okuma, K. Mae, *Energy Fuels* **2004**, *18*, 755.
[64] S. Azhar, *Doctoral Thesis*, KTH Royal Institute of Technology, Stockholm, Sweden **2015**; avaliable from https://www.diva-portal.org/smash/get/diva2:781407/FULLTEXT01.pdf.
[65] M. Saska, E. Ozer, *Biotechnol. Bioeng.* **1995**, *45*, 517.
[66] C. Froschauer, M. Hummel, M. Iakovlev, A. Roselli, H. Schottenberger, H. Sixta, *Biomacromolecules* **2013**, *14*, 1741.
[67] F.-Z. Belmokaddem, C. Pinel, P. Huber, M. Petit-Conil, D. D. S. Perez, *Carbohydr. Res.* **2011**, *346*, 2896.
[68] J. Ren, R. Sun, C. Liu, Z. Cao, W. Luo, *Carbohydr. Polym.* **2007**, *70*, 406.
[69] X. F. Sun, R. C. Sun, J. X. Sun, *J. Sci. Food Agric.* **2004**, *84*, 800.
[70] I. Woodward, W. Schofield, V. Roucoules, J. Badyal, *Langmuir* **2003**, *19*, 3432.
[71] J. Pourchez, A. Govin, P. Grosseau, R. Guyonnet, B. Guilhot, B. Ruot, *Cem. Concr. Res.* **2006**, *36*, 1252.
[72] A. Salam, R. A. Venditti, J. J. Pawlak, K. El-Tahlawy, *Carbohydr. Polym.* **2011**, *84*, 1221.
[73] G. S. Kelly, *Alternat. Med. Rev.: J. Clin. Ther.* **1999**, *4*, 96.
[74] V. Apostolopoulos, G. A. Pietersz, A. Tsibanis, A. Tsikkinis, H. Drakaki, B. E. Loveland, S. J. Piddlesden, M. Plebanski, D. S. Pouniotis, M. N. Alexis, *Breast Cancer Res.* **2006**, *8*, R27.
[75] C. K. Tang, K.-C. Sheng, S. E. Esparon, O. Proudfoot, V. Apostolopoulos, G. A. Pietersz, *Biomaterials* **2009**, *30*, 1389.
[76] N. Sharon, *Biochim. Biophys. Acta, Gen. Subj.* **2006**, *1760*, 527.
[77] L. Iwamoto, T. Watanabe, A. Ogasawara, T. Mikami, T. Matsumoto, *Yakugaku Zasshi* **2006**, *126*, 167.
[78] a) L. M. Ferreira, C. S. Sobral, L. Blanes, M. Z. Ipolito, E. K. Horibe, *J. Plast., Reconstr. Aesthetic Surg.* **2010**, *63*, 865; b) D. Melandri, A. De Angelis, R. Orioli, G. Ponzielli, P. Lualdi, N. Giarratana, V. Reiner, *Burns* **2006**, *32*, 964.
[79] N. Kulkarni, A. Shendye, M. Rao, *FEMS Microbiol. Rev.* **1999**, *23*, 411.
[80] U. Edlund, A.-C. Albertsson, *J. Bioact. Compat. Polym.* **2008**, *23*, 171.
[81] B. Jiang, L. Hu, C. Gao, J. Shen, *Acta Biomater.* **2006**, *2*, 9.
[82] K. S. Mikkonen, M. Tenkanen, *Trends Food Sci. Technol.* **2012**, *28*, 90.
[83] O. Gordobil, I. Egüés, I. Urruzola, J. Labidi, *Carbohydr. Polym.* **2014**, *112*, 56.
[84] P. Gatenholm, A. Bodin, M. Gröndahl, S. Dammstrom, L. Eriksson, *US 7427643B2*, **2008**.
[85] M. Gröndahl, L. Bindgard, P. Gatenholm, T. Hjertberg, *US 2014/0093724 A1*, **2013**.
[86] C. Peroval, F. Debeaufort, A.-M. Seuvre, B. Chevet, D. Despre, A. Voilley, *J. Agric. Food Chem.* **2003**, *51*, 3120.
[87] H. M. Shaikh, K. V. Pandare, G. Nair, A. J. Varma, *Carbohydr. Polym.* **2009**, *76*, 23.
[88] V. Kisonen, C. Xu, R. Bollström, J. Hartman, H. Rautkoski, M. Nurmi, J. Hemming, P. Eklund, S. Willför, *Cellulose* **2014**, *21*, 4497.
[89] D. Kun, B. Pukánszky, *Eur. Polym. J.* **2017**, *93*, 618.
[90] A. Grossman, W. Vermerris, *Curr. Opin. Biotechnol.* **2019**, *56*, 112.
[91] J. Zhu, C. Yan, X. Zhang, C. Yang, M. Jiang, X. Zhang, *Prog. Energy Combust. Sci.* **2020**, *76*, 100788.

[92] Z. Wang, M. S. Ganewatta, C. Tang, *Prog. Polym. Sci.* **2019**, 101197.
[93] P. Figueiredo, K. Lintinen, J. T. Hirvonen, M. A. Kostiainen, H. A. Santos, *Prog. Mater. Sci.* **2018**, *93*, 233.
[94] R. Rinaldi, R. Jastrzebski, M. T. Clough, J. Ralph, M. Kennema, P. C. Bruijnincx, B. M. Weckhuysen, *Angew. Chem., Int. Ed.* **2016**, *55*, 8164.
[95] D. Cao, Q. Zhang, A. M. Hafez, Y. Jiao, Y. Ma, H. Li, Z. Cheng, C. Niu, H. Zhu, *Small Methods* **2019**, *3*, 1800539.
[96] S.-D. Gong, Y. Huang, H.-J. Cao, Y.-H. Lin, Y. Li, S.-H. Tang, M.-S. Wang, X. Li, *J. Power Sources* **2016**, *307*, 624.
[97] H. Lu, A. Cornell, F. Alvarado, M. Behm, S. Leijonmarck, J. Li, P. Tomani, G. Lindbergh, *Materials* **2016**, *9*, 127.
[98] L. Du, W. Wu, C. Luo, D. Xu, H. Guo, R. Wang, T. Zhang, J. Wang, Y. Deng, *J. Electrochem. Soc.* **2019**, *166*, A423.
[99] A. Mukhopadhyay, J. Hamel, R. Katahira, H. Zhu, *ACS Sustainable Chem. Eng.* **2018**, *6*, 5394.
[100] a) F. Chen, Y. Tobimatsu, D. Havkin-Frenkel, R. A. Dixon, J. Ralph, *Proc. Natl. Acad. Sci. USA* **2012**, *109*, 1772; b) Y. Li, L. Shuai, H. Kim, A. H. Motagamwala, J. K. Mobley, F. Yue, Y. Tobimatsu, D. Havkin-Frenkel, F. Chen, R. A. Dixon, *Sci. Adv.* **2018**, *4*, eaau2968.
[101] a) Q. Abbas, F. Béguin, *J. Power Sources* **2016**, *318*, 235; b) H. Yu, J. Wu, L. Fan, K. Xu, X. Zhong, Y. Lin, J. Lin, *Electrochim. Acta* **2011**, *56*, 6881.
[102] a) S. Herou, M. C. Ribadeneyra, R. Madhu, V. Araullo-Peters, A. Jensen, P. Schlee, M. Titirici, *Green Chem.* **2019**, *21*, 550; b) P. Schlee, S. Herou, R. Jervis, P. R. Shearing, D. J. Brett, D. Baker, O. Hosseinaei, P. Tomani, M. M. Murshed, Y. Li, *Chem. Sci.* **2019**, *10*, 2980.
[103] G. Milczarek, O. Inganäs, *Science* **2012**, *335*, 1468.
[104] J. W. Jeon, L. Zhang, J. L. Lutkenhaus, D. D. Laskar, J. P. Lemmon, D. Choi, M. I. Nandasiri, A. Hashmi, J. Xu, R. K. Motkuri, *ChemSusChem* **2015**, *8*, 428.
[105] a) W. O. Doherty, P. Mousavioun, C. M. Fellows, *Ind. Crops Prod.* **2011**, *33*, 259; b) S. S. Nair, S. Sharma, Y. Pu, Q. Sun, S. Pan, J. Zhu, Y. Deng, A. J. Ragauskas, *ChemSusChem* **2014**, *7*, 3513.
[106] W. Zhao, B. Simmons, S. Singh, A. Ragauskas, G. Cheng, *Green Chem.* **2016**, *18*, 5693.
[107] D. Kai, M. J. Tan, P. L. Chee, Y. K. Chua, Y. L. Yap, X. J. Loh, *Green Chem.* **2016**, *18*, 1175.
[108] a) C. Thulluri, S. R. Pinnamaneni, P. R. Shetty, U. Addepally, *Ind. Biotechnol.* **2016**, *12*, 153; b) Q. Li, S. Xie, W. K. Serem, M. T. Naik, L. Liu, J. S. Yuan, *Green Chem.* **2017**, *19*, 1628; c) Q. Li, M. T. Naik, H.-S. Lin, C. Hu, W. K. Serem, L. Liu, P. Karki, F. Zhou, J. S. Yuan, *Carbon* **2018**, *139*, 500.
[109] a) Q. Lu, M. Zhu, Y. Zu, W. Liu, L. Yang, Y. Zhang, X. Zhao, X. Zhang, X. Zhang, W. Li, *Food Chem.* **2012**, *135*, 63; b) S. R. Yearla, K. Padmasree, *J. Exp. Nanosci.* **2016**, *11*, 289; c) C. Liu, Y. Li, Y. Hou, *Eur. Polym. J.* **2019**, *112*, 15; d) C. Liu, Y. Li, Y. Hou, *eXPRESS Polym. Lett.* **2018**, *12*, 946.
[110] A. P. Richter, J. S. Brown, B. Bharti, A. Wang, S. Gangwal, K. Houck, E. A. C. Hubal, V. N. Paunov, S. D. Stoyanov, O. D. Velev, *Nat. Nanotechnol.* **2015**, *10*, 817.
[111] E. D. Bartzoka, H. Lange, K. Thiel, C. Crestini, *ACS Sustainable Chem. Eng.* **2016**, *4*, 5194.
[112] X. Liu, H. Yin, Z. Zhang, B. Diao, J. Li, *Colloids Surf., B* **2015**, *125*, 230.
[113] a) H. M. Caicedo, L. A. Dempere, W. Vermerris, *Nanotechnology* **2012**, *23*, 105605; b) E. Ten, C. Ling, Y. Wang, A. Srivastava, L. A. Dempere, W. Vermerris, *Biomacromolecules* **2014**, *15*, 327.
[114] C. Liu, Y. Li, Y. Hou, *Molecules* **2019**, *24*, 2704.
[115] a) D. Y. Leung, G. Caramanna, M. M. Maroto-Valer, *Renewable Sustainable Energy Rev.* **2014**, *39*, 426; b) Y. Sun, G. Sun, V. Sage, Z. Sun, J. p. Zhang, L. Zhang, *Environ. Prog. Sustainable Energy* **2017**, *36*, 1417.
[116] D. Saha, S. E. Van Bramer, G. Orkoulas, H.-C. Ho, J. Chen, D. K. Henley, *Carbon* **2017**, *121*, 257.
[117] a) D. Bilba, D. Suteu, T. Malutan, *Open Chem.* **2008**, *6*, 258; b) S. Zhang, Z. Wang, Y. Zhang, H. Pan, L. Tao, *Procedia Environ. Sci.* **2016**, *31*, 3; c) D. Mohan, A. Sarswat, Y. S. Ok, C. U. Pittman Jr., *Bioresour. Technol.* **2014**, *160*, 191.
[118] K. Fu, Q. Yue, B. Gao, Y. Sun, L. Zhu, *Chem. Eng. J.* **2013**, *228*, 1074.
[119] Y. Ge, Z. Li, *ACS Sustainable Chem. Eng.* **2018**, *6*, 7181.
[120] N. Supanchaiyamat, K. Jetsrisuparb, J. T. Knijnenburg, D. C. Tsang, A. J. Hunt, *Bioresour. Technol.* **2019**, *272*, 570.
[121] G. G. Dossa, E. Paudel, K. Cao, D. Schaefer, R. D. Harrison, *Sci. Rep.* **2016**, *6*, 34153.
[122] N. A. Rosdiana, S. Dumarçay, C. Gérardin, H. Chapuis, F. J. Santiago-Medina, R. K. Sari, W. Syafii, E. Gelhaye, P. Raharivelomanana, R. Mohammed, *Ind. Crops Prod.* **2017**, *108*, 121.
[123] L. Gil, *Materials* **2015**, *8*, 625.
[124] J. D'Souza, N. Yan, *ACS Sustainable Chem. Eng.* **2013**, *1*, 534.
[125] W. Chen, N. Li, Y. Ma, M. L. Minus, K. Benson, X. Lu, X. Wang, X. Ling, H. Zhu, *Biomacromolecules* **2019**, *20*, 4476.
[126] A. Mukhopadhyay, Y. Jiao, R. Katahira, P. N. Ciesielski, M. Himmel, H. Zhu, *Nano Lett.* **2017**, *17*, 7897.
[127] Y. Zhao, N. Yan, M. W. Feng, *ACS Sustainable Chem. Eng.* **2013**, *1*, 91.
[128] a) Y. Zhao, N. Yan, M. Feng, *J. Appl. Polym. Sci.* **2012**, *123*, 2849; b) T. Ueno, *Mokuzai Kogyo* **2007**, *62*, 358; c) Z. Xue, X. Zhao, R.-c. Sun, T. Mu, *ACS Sustainable Chem. Eng.* **2016**, *4*, 3864; d) P.-Y. Kuo, M. Sain, N. Yan, *Green Chem.* **2014**, *16*, 3483.
[129] F. Melone, R. Saladino, H. Lange, C. Crestini, *J. Agric. Food Chem.* **2013**, *61*, 9316.
[130] G. D. Scholes, G. R. Fleming, A. Olaya-Castro, R. Van Grondelle, *Nat. Chem.* **2011**, *3*, 763.
[131] a) R. M. Maxwell, L. E. Condon, *Science* **2016**, *353*, 377; b) S. P. Good, D. Noone, G. Bowen, *Science* **2015**, *349*, 175.
[132] a) F. Qa'dan, A.-J. Thewaini, D. A. Ali, R. Afifi, A. Elkhawad, K. Z. Matalka, *Am. J. Chin. Med.* **2005**, *33*, 197; b) M. Adamu, V. Naidoo, J. N. Eloff, *BMC Vet. Res.* **2014**, *10*, 52.
[133] V. Manikandan, P. Velmurugan, J.-H. Park, N. Lovanh, S.-K. Seo, P. Jayanthi, Y.-J. Park, M. Cho, B.-T. Oh, *Mater. Lett.* **2016**, *185*, 335.
[134] A. Sharma, K. G. Bhattacharyya, *J. Hazard. Mater.* **2005**, *125*, 102.
[135] Y. P. Kumar, P. King, V. Prasad, *J. Hazard. Mater.* **2006**, *137*, 1211.
[136] S. H. Chung, A. Manthiram, *ChemSusChem* **2014**, *7*, 1655.
[137] A. K. Mondal, K. Kretschmer, Y. Zhao, H. Liu, C. Wang, B. Sun, G. Wang, *Chem. - Eur. J.* **2017**, *23*, 3683.
[138] Y. Jie, X. Jia, J. Zou, Y. Chen, N. Wang, Z. L. Wang, X. Cao, *Adv. Energy Mater.* **2018**, *8*, 1703133.
[139] S. Zhuang, L. Zhou, W. Xu, N. Xu, X. Hu, X. Li, G. Lv, Q. Zheng, S. Zhu, Z. Wang, *Adv. Sci.* **2018**, *5*, 1700497.
[140] A. M. Awwad, N. M. Salem, A. O. Abdeen, *Adv. Mater. Lett.* **2013**, *4*, 338.
[141] a) Y.-C. Liu, L.-H. Lin, *Electrochem. Commun.* **2004**, *6*, 1163; b) C. H. Bae, S. H. Nam, S. M. Park, *Appl. Surf. Sci.* **2002**, *197–198*, 628; c) Z. Khan, S. A. Al-Thabaiti, A. Y. Obaid, A. Al-Youbi, *Colloids Surf., B* **2011**, *82*, 513.
[142] A. M. Awwad, B. Albiss, *Adv. Mater. Lett.* **2015**, *6*, 51.
[143] C. Singh, R. K. Baboota, P. K. Naik, H. Singh, *Adv. Mater. Lett.* **2012**, *3*, 279.
[144] B. Ankamwar, C. Damle, A. Ahmad, M. Sastry, *J. Nanosci. Nanotechnol.* **2005**, *5*, 1665.
[145] S. Shalini, S. Prasanna, T. K. Mallick, S. Senthilarasu, *Renewable Sustainable Energy Rev.* **2015**, *51*, 1306.
[146] W. A. Ayalew, D. W. Ayele, *J. Sci.: Adv. Mater. Devices* **2016**, *1*, 488.
[147] C. Li, H. Du, L. Wang, Q. Shu, Y. Zheng, Y. Xu, J. Zhang, J. Zhang, R. Yang, Y. Ge, *J. Agric. Food Chem.* **2009**, *57*, 8496.
[148] H. Hug, M. Bader, P. Mair, T. Glatzel, *Appl. Energy* **2014**, *115*, 216.
[149] A. R. Hernandez-Martinez, M. Estevez, S. Vargas, F. Quintanilla, R. Rodriguez, *Int. J. Mol. Sci.* **2011**, *12*, 5565.
[150] A. Mukhopadhyay, H. Zhao, B. Li, J. Hamel, Y. Yang, D. Cao, A. Natan, H. Zhu, *ACS Appl. Energy Mater.* **2019**, *2*, 7425.

[151] F. Wu, J. Gao, X. Zhai, M. Xie, Y. Sun, H. Kang, Q. Tian, H. Qiu, *Carbon* **2019**, *147*, 242.
[152] S. Senthilkumaar, P. Kalaamani, C. Subburaam, *J. Hazard. Mater.* **2006**, *136*, 800.
[153] A. Kumar, S. Sharma, *Ind. Crops Prod.* **2008**, *28*, 1.
[154] A. Warra, *Am. J. Sci. Ind. Res.* **2012**, *3*, 358.
[155] N. Yi, Z. Cheng, L. Yang, G. Edelman, C. Xue, Y. Ma, H. Zhu, H. Cheng, *ACS Appl. Mater. Interfaces* **2018**, *10*, 36664.
[156] M. Premalatha, T. Mathavan, S. Selvasekarapandian, S. Monisha, D. V. Pandi, S. Selvalakshmi, *J. Non-Cryst. Solids* **2016**, *453*, 131.
[157] R. Srinivasan, E. Elaiyappillai, H. P. Pandian, R. Vengudusamy, P. M. Johnson, S.-M. Chen, R. Karvembu, *J. Electroanal. Chem.* **2019**, *849*, 113382.
[158] S. Gueu, B. Yao, K. Adouby, G. Ado, *J. Appl. Sci.* **2006**, *6*, 2789.
[159] S. Mane, A. Vanjara, M. Sawant, *J. Chin. Chem. Soc.* **2005**, *52*, 1117.
[160] I. Brunner, D. L. Godbold, *J. Forest Res.* **2007**, *12*, 78.
[161] C. Zhang, X. Zhou, J. Jiang, Y. Wei, J. Ma, P. D. Hallett, *Catena* **2019**, *172*, 140.
[162] a) S. Sochacki, P. Ritson, B. Brand, R. Harper, B. Dell, *Ecol. Eng.* **2017**, *98*, 264; b) O. Forey, F. Temani, J. Wery, C. Jourdan, A. Metay, *Eur. J. Agron.* **2017**, *91*, 16.
[163] A. Sanchez-Sanchez, M. T. Izquierdo, J. Ghanbaja, G. Medjahdi, S. Mathieu, A. Celzard, V. Fierro, *J. Power Sources* **2017**, *344*, 15.
[164] H. A. Bacelo, S. C. Santos, C. M. Botelho, *Chem. Eng. J.* **2016**, *303*, 575.
[165] N. R. Kim, H. J. An, Y. S. Yun, H.-J. Jin, *Carbon Lett.* **2017**, *22*, 110.
[166] E. Hao, W. Liu, S. Liu, Y. Zhang, H. Wang, S. Chen, F. Cheng, S. Zhao, H. Yang, *J. Mater. Chem. A* **2017**, *5*, 2204.
[167] S. Machado, J. Pacheco, H. Nouws, J. T. Albergaria, C. Delerue-Matos, *Sci. Total Environ.* **2015**, *533*, 76.
[168] a) W. Ai, W. Zhou, Z. Du, C. Sun, J. Yang, Y. Chen, Z. Sun, S. Feng, J. Zhao, X. Dong, *Adv. Funct. Mater.* **2017**, *27*, 1603603; b) J. Yang, Y. Yang, A. Li, Z. Wang, H. Wang, D. Yu, P. Hu, M. Qian, J. Lin, L. Guo, *Energy Storage Mater.* **2019**, *17*, 334.
[169] R. P. Panmand, P. Patil, Y. Sethi, S. R. Kadam, M. V. Kulkarni, S. W. Gosavi, N. Munirathnam, B. B. Kale, *Nanoscale* **2017**, *9*, 4801.
[170] X. Li, H. Xu, *ChemistrySelect* **2018**, *3*, 10624.
[171] M. U. Ashraf, M. A. Hussain, S. Bashir, M. T. Haseeb, Z. Hussain, *J. Drug Delivery Sci. Technol.* **2018**, *45*, 455.
[172] B. Sivasankari, M. Anandharaj, P. Gunasekaran, *J. Ethnopharmacol.* **2014**, *153*, 408.